LA-3064

LA-3064

LOS ALAMOS SCIENTIFIC LABORATORY
OF THE UNIVERSITY OF CALIFORNIA o LOS ALAMOS   NEW MEXICO

THEORY OF THE FIREBALL

20001031 133

LEGAL NOTICE

LOS ALAMOS SCIENTIFIC LABORATORY
OF THE UNIVERSITY OF CALIFORNIA   LOS ALAMOS   NEW MEXICO

THEORY OF THE FIREBALL

by

Hans A. Bethe

ABSTRACT

The successive stages of the fireball due to a nuclear explosion in air are defined (Sec. 2). This paper is chiefly concerned with Stage C, from the minimum in the apparent fireball temperature to the point where the fireball becomes transparent. In the first part of this stage (C I), the shock (which previously was opaque) becomes transparent due to decreasing pressure. The radiation comes from a region in which the temperature distribution is given essentially by the Taylor solution; the radiating layer is given by the condition that the mean free path is about 1/50 of the radius (Sec. 3). The radiating temperature during this stage increases about as $p^{-1/4}$, where p is the pressure.

To supply the energy for the radiation, a cooling wave proceeds from the outside into the hot interior (Sec. 5). When this wave reaches the isothermal sphere, the temperature is close to its second maximum. Thereafter, the character of the solution changes; it is now dominated by the cooling wave (Stage C II). The temperature would decrease slowly (as $p^{1/6}$) if the problem were one-dimensional, but in fact it is probably nearly constant for the three-dimensional case (Sec. 6). The radiating surface shrinks slowly. The cooling wave eats into the isothermal sphere until this is completely used up. The inner part of the isothermal sphere,

3

i.e., the part which has not yet been reached by the cooling wave, continues to expand adiabatically; it therefore cools very slowly and remains opaque.

After the entire isothermal sphere is used up, the fireball becomes transparent and the radiation drops rapidly. The ball will therefore be left at a rather high temperature (Sec. 7), about 5000°.

The cooling wave reaches the isothermal sphere at a definite pressure $p_c \approx 5(\rho_1/\rho_0)^{1/3}$ bars, where ρ_1 is the ambient and ρ_0 the sea level density. The radiating temperature at this time is about $10,000^{\circ}$. The slight dependence of physical properties on yield is exhibited in approximate formulae.

ACKNOWLEDGEMENTS

CONTENTS

1. INTRODUCTION

The radiation from the fireball has been studied intensively by many authors. Already in the Summer Study at Berkeley in 1942, Bethe and Teller[1] found that the energy transmitted by a nuclear explosion into air is immediately converted into x-rays, and studied the qualitative features of the transmission of these x-rays. At Los Alamos, Marshak[2] and others showed that this radiation propagates as a wave, with a sharp front. Hirschfelder and Magee[3] gave the first comprehensive treatment of this early phase of the fireball development, and also studied some of the later phases, especially the role of NO_2.

Many optical observations have been made in the numerous tests of atomic weapons. Some of the results are contained in "Effects of Nuclear Weapons,"[4] pp. 70-84 (see also pp. 316-368). A summary of the spectroscopic observations up to 1956 was compiled by DeWitt.[5] Careful scrutiny of the extensive observational material would undoubtedly give a wealth of further information.

On the theoretical side, there has been some analytical and a good deal of numerical work. Analytical work has concentrated on the early phases. One of the most recent analytical papers on the early flow of

radiation (Stage A of Sec. 2) is by Freeman.[6] Brode and Gilmore[7] treat
also Stage B, the radiation from the shock front, with particular emphasis
on the dependence on altitude.

The most complete numerical calculation has been done by Brode[8] on
a sea level megaton explosion. We shall use his results extensively,
but for convenience we shall translate them to a yield of 1 megaton.
Wherever the phenomena are purely hydrodynamic, we may simply scale the
linear dimensions and the time by the cube root of the yield, and this
is the principal use we shall make of Brode's results, e.g. in Sec. 3b.
Where radiation is important, this scaling will give only a rough guide.
Brode calculates pressures, temperatures, densities, etc., as functions
of time and radius, for scaled (1-megaton) times of about 10^{-7} to 10
seconds. The calculations show clearly the stages in fireball and shock
development, as defined in Sec. 2, at least Stages A to C.

Brode and Meyerott[9] have considered the physical phenomena involved
in the optical "opening" of the shock after the minimum of radiation,
Stage C I in the nomenclature of Sec. 2, especially the decrease in
opacity due to decreased density and to the dissociation of NO_2.

Zel'dovich, Kompaneets and Raizer[10] have investigated how the energy
for the radiation is supplied after the radiation minimum and have intro-
duced the concept of a "cooling wave" moving into the hot fireball. The
present report is largely concerned with an extension of the ideas of
Zel'dovich et al. to the actual case of density varying with time, more
general opacity function, radiation absorption varying with wave length,
etc.

Much effort has been devoted to the calculation of fireballs at various altitudes. Brode[11] made such calculations in 1958, in connection with the test series of that year. Gilmore[12] made a prediction of the Bluegill explosion in 1962. Since then, many more refined calculations of Bluegill have been made.

For any understanding of fireball phenomena it is essential to have a good equation of state for air and good tables of absorption coefficients. For the equation of state, we have used Gilmore's tables,[13] although Hilsenrath's[14] give more detail in some respects. The two calculations agree. Gilmore's equation was approximated analytically by Brode.[8]

For the absorption coefficient we have used the tables by Meyerott et al.,[15,16] which extend to 12,000°. These were supplemented by the work of Kivel and Bailey[17] and more recent work by Taylor and Kivel[18] on the free-free electron transitions in the field of neutral atoms and molecules. At higher temperatures, there are calculations by Gilmore and Latter,[19] Karzas and Latter,[20] and curves by Gilmore[21] which are brought up to date periodically. The most recent calculation on the absorption of air at about 18,000° and above have been done by Stuart and Pyatt.[22] This temperature range is not of great importance for the problem of this paper, but is important for the expansion of the isothermal sphere inside the shock wave before it is reached by the cooling wave.

Brode[8] has used the average of the absorption coefficient over

frequency, the opacity, which is sufficient for treating the internal flow of radiation. A realistic treatment of the flow to the outside requires the absorption coefficient as a function of frequency; Brode merely wanted to obtain reasonable overall results for this flow. He approximated the opacity by an analytic expression. Also in most of the other work cited above an average opacity has been used. An exception is some of the recent work on the radiation flow in high altitude explosions (Bluegill), where the frequency dependence must be, and has been, taken into account. Gilmore[21] has calculated and made available curves of effective opacity, in which the radiation mean free path was averaged (using a Rosseland weighting factor) only over those frequencies for which it is less than 1 kilometer.

This list of references on work on the fireball dynamics and opacity is far from complete.

2. PHASES IN DEVELOPMENT

The energy from a nuclear explosion is transmitted through the outer parts of the weapon, including its case, either by radiation (x-rays) or by shock or both. Whichever the mode of transmission inside the weapon, once the energy gets into the surrounding air, the energy will be transported by x-rays. This is because the air will be heated to such a high temperature (a million degrees or more) that transport by x-rays is much faster than by hydrodynamics. This stage of energy transport (Stage A) has been extensively studied by many authors (e.g., Hirschfelder and

12

Magee in Report LA-2000) and will therefore not be further considered here.

During Stage A, temperatures are very high. The Planck spectrum of the air is in the x-ray or far ultraviolet region, and hence is immediately absorbed by the surrounding air. The very hot air is therefore surrounded by a cooler envelope, and only this envelope is visible to observers at a distance. The observable temperature therefore has little physical significance. It is observed that the size of the luminous sphere increases rapidly, and the total emission also increases, up to a first maximum.

When the temperature of the central sphere of air has fallen, by successive emission and re-absorption of x-rays, to about $300,000^\circ$, a hydrodynamic shock forms. The shock now moves faster than the temperature could propagate by radiation transport. The shock therefore separates from the very hot, nearly isothermal sphere at the center. This is Stage B in the development. The shock moves by simple hydrodynamics. Its front obeys the Hugoniot relations, the density being given by (3.4). Behind the front, the air expands adiabatically, and at a radius of 80% of the shock radius, the density is apt to have fallen by a factor of 10 or more compared to the shock density, while the temperature has risen by a comparable factor, (3.16). Thus the interior is at very low density, and hence the pressure must be nearly constant (otherwise there would be very large accelerations which soon would equalize the pressure). This greatly simplifies the structure of the shock, and leads to such simple

relations as (3.2) between shock radius and pressure.

Well inside the shock, the "isothermal sphere" pursues its separate history. It continues to engulf more material because radiation flow continues, though at a reduced rate. H. Brode has kindly calculated for me the temperature histories of several material points, based on his paper RM-2248. These histories clearly exhibit the expansion of the isothermal sphere in material coordinates. The expansion can also be treated by a semi-analytic method which I hope to discuss in a subsequent paper. The isothermal sphere remains isolated from the outside world until it is reached by the cooling wave, Sec. 5.

The radiation to the outside now comes from the shock. Early in Stage B, the shock has a precursor of lower temperature, caused by ultra-violet radiation from the shock, and the observable temperature is still below the shock temperature (Stage B I). However, the observable radius is very near the shock radius. Later, as the shock front cools down, the shock radiates directly and its temperature becomes directly observable (Stage B II). The first maximum in visible radiation probably occurs between Stages B I and B II. As the shock cools down, the radiation from the shock front decreases, and the observable temperature decreases to a minimum (Ref. 4, par. 2.113, p. 75) of about 2000°.

When the shock is sufficiently cool, its front becomes transparent, and one can look into it to higher temperatures (Stage C). The central isothermal sphere, however, remains opaque and, for some time, invisible. Because higher temperatures are now revealed, the total radiation increases

14

toward a second maximum. This stage has been very little considered theoretically, except in numerical calculations, and forms the subject of this report.

We shall show that for some time in Stage C, the radiation comes from the air between isothermal sphere and shock front (Stage C I). During this time, the radiation can be calculated essentially from the temperature distribution which is set up by the adiabatic expansion of the material behind the shock (Secs. 3 and 5f,g). The temperature and total intensity of the radiation increase with time toward the larger, second maximum.

The energy for the radiation is largely supplied by a cooling wave (Sec. 5) which gradually eats into the hot interior. When this cooling wave reaches the isothermal sphere, the radiation temperature reaches its maximum (Sec. 5e); it then declines again as the cooling wave eats more deeply into the isothermal sphere (Stage C II). This process ends by the isothermal sphere being completely eaten away (Sec. 6).

After this has happened, the entire fireball, isothermal sphere and cooler envelope, is transparent to its own thermal radiation (Stage D). The molecular bands, which previously appeared in absorption, now appear in emission (Stage D I). Emission will lead to further cooling of the fireball, though more slowly than before. Soon, when the temperature falls below about 6000°, the emission becomes very weak, and subsequent cooling is almost entirely adiabatic (Stage D II). At sea level, the pressure may go down to 1 bar before the temperature falls below 6000°;

15

in this case there is no Stage D II. At higher elevation, there usually is.

The fireball will then remain hot, at about 6000° or a somewhat lower temperature due to adiabatic expansion in Stage D II. The only process which can now lead to further cooling is the rise of the fireball, which leads to further adiabatic expansion and, more important, to turbulent mixing at the surface with the ambient air (Stage E). The time required for this is typically 10 seconds or more, being determined by buoyancy.

At very high altitude, the shock wave never plays an important part, but radiation transport continues until the temperature gets too low for effective emission. In other words, Stage A continues to the end. Of course, a shock does form, but it is, so to speak, an afterthought, and it plays little part in the distribution of energy. At medium altitude, let us say, 10 to 30 kilometers, the stages are much the same as at sea level but the shock wave becomes transparent earlier, i.e., at a higher temperature, because the density is lower; this means that the minimum emission comes earlier. Stage C proceeds similarly to sea level, but at the second maximum of radiation the pressure is still much above ambient, therefore Stage C II involves a greater radial expansion of the isothermal sphere than at sea level which proceeds simultaneously with the inward motion of the cooling wave. Moreover, there is much adiabatic expansion after the cooling wave has penetrated to the center. The temperature at which radiation stops is higher, due to the lower density.

We believe that the theory developed in this paper will be useful in studying the dependence of phenomena on altitude (ambient pressure), but we have not yet exploited it for this purpose.

3. RADIATION FROM BEHIND THE SHOCK (Stage C I)

a. Role of NO_2

The diatomic species in equilibrium air, both neutrals and ions, show very little absorption in the visible at temperatures up to about $4000^\circ K$. This is shown clearly in the tables by Meyerott et al.[16] We define "the visible" for the purposes of this paper, arbitrarily and incorrectly, as the frequency range

$$h\nu = 1/2 \text{ to } 2\text{-}3/4 \text{ ev}$$

$$= 4050 \text{ to } 22,300 \text{ cm}^{-1}$$

$$= 2.48 \text{ to } 0.45 \; \mu \tag{3.1}$$

Then, even at a density as high as $10\rho_0$ (ρ_0 = density of air at NTP $= 1.29 \times 10^{-3} \text{ gm/cm}^3$), the mean free path is never less than 100 meters at 4000°, 1000 meters at 3000°, and still longer at lower temperature. These values refer to $h\nu = 2\text{-}5/8$ ev; for lower frequencies, the mean free path is even longer.

In the sea-level shock wave from a megaton explosion, the temperature range from 3000 to 4000° occupies a distance of about 10 meters (see Sec. 3b). Thus this region is definitely transparent, even at the

highest possible density of about $10\rho_0$. For explosions at higher altitude, this conclusion is even more true.

The tables by Meyerott et al. do not include absorption by triatomic (and more complicated) molecules. Of these, NO_2 is known to have strong absorption bands in the visible. After this paper was completed, I received new calculations by Gilmore[23] which include the effect of NO_2. The effect is very striking as is shown by Table I, which gives the absorption coefficient for the "typical" frequency $h\nu = 2\text{-}1/8$ ev, and for several temperatures and densities (the absorption is strong from about 1-3/4 to 2-3/4 ev).

Table I. Absorption Coefficients at $h\nu = 2\text{-}1/8$ ev
with and without NO_2

ρ/ρ_0	10	10	10	10	1
T	2000	3000	4000	6000	3000
Without	0	1.7^{-8}	8.3^{-6}	3.1^{-2}	1.7^{-9}
With	5.3^{-3}	1.2^{-2}	1.5^{-2}	3.1^{-2}	3.7^{-4}

Note: For each value, the power of 10 is indicated by a superscript.

Because NO_2 is triatomic, its absorption depends strongly on density. As the shocked gas expands, the NO_2 dissociates and the gas becomes transparent. Brode and Meyerott[9] have calculated, under reasonable assumptions, the effect of this dissociation on the optical properties of the fireball. We shall not discuss the effect of NO_2 any further, but shall assume that this substance has almost disappeared by the time we are considering.

18

b. Temperature Distribution behind the Shock

We wish to calculate the temperature distribution behind the shock.
We can do this because the material which has gone through the shock
expands very nearly adiabatically, as long as it is not engulfed by the
internal, hot isothermal sphere. We are interested in the period when
the shock temperature goes from about 4000 to a few hundred degrees, i.e.,
until the strong cooling wave (Sec. 5) starts. For a 1-megaton explosion,
this corresponds roughly to t = 0.05 to 0.25 second.

At a given time, the pressure is nearly constant over most of the
volume inside the shock, except for the immediate neighborhood of the
shock; the shock pressure is roughly twice this constant, inside pressure.
Comparing two material elements in the "inside" region, we may calculate
their relative temperatures if we know their temperatures when the shock
traversed them, and assume adiabatic expansion from there on.

A material element which is initially at point r will be shocked
when the shock radius is r. The shock pressure at this time is[*]

$$P_s(r) = 20(\gamma'_{Av} - 1)Yr^{-3} \tag{3.2}$$

where

    Y = yield in megatons

    r = radius in kilometers

$$\gamma' - 1 = \frac{P}{\rho E} = \frac{\text{pressure}}{\text{energy per unit volume}} \tag{3.3}$$

---

[*]Notations for thermodynamic quantities similar to those of Gilmore
(Report RM-1543).

and the average of γ' is taken over the volume inside the shock wave. The basis of (3.2) is that the total energy in the shocked volume, Y, is the volume times the average energy per unit volume, the latter is the average pressure divided by $\gamma' - 1$, and the average pressure is close to one-half of the shock pressure.

The density at the shock is

$$\rho_s = \frac{\gamma'_s + 1}{\gamma'_s - 1} \rho_0 \approx \frac{2}{\gamma'_s - 1} \rho_0 \tag{3.4}$$

where the subscript s refers to shock conditions. Now an examination of Gilmore's tables[13] shows that γ' does not change very much along an adiabat. As an example, we list in Table II certain quantities referring to some adiabats which will be particularly important for our theory. These are the adiabats for which the temperature T is between 4000 and 12,000° at a density of $0.1\rho_0$. In the second line we list the temperature T_s for the same entropy S at a density $\rho_s = 10\rho_0$. This is close enough to the shock density (3.4) so we may consider T_s as the temperature of the same material when the shock wave went through it. (Adiabatic expansion, i.e., no radiation transport, is assumed.) The third line gives $\gamma' - 1$ for the "present" conditions, $\rho = 0.1\rho_0$ and T, the fourth line is the same quantity for the shock conditions. It is evident that $\gamma' - 1$ is nearly constant for T = 4000 and 6000°, not so constant for 8000 and 12,000°. On the average $\gamma' - 1 \approx 0.18$. The last two lines in Table II give the number of particles (atoms, ions, electrons) per original air molecule under "present" and shock conditions.

Table II. Adiabats

("Present" density, $0.1\rho_0$; shock density, $10\rho_0$)

T	4,000	6,000	8,000	12,000
T_s	9,000	10,500	18,000	28,000
$\gamma' - 1$	0.213	0.194	0.144	0.153
$\gamma'_s - 1$	0.208	0.190	0.190	0.20
Z	1.13	1.27	1.68	2.06
Z_s	1.3	1.6	2.06	3

Assuming an adiabat of constant $\gamma = \gamma'$, the density of a mass element is

$$\rho = \rho_s \left(\frac{p}{p_s}\right)^{1/\gamma} \tag{3.5}$$

Now ρ_s is a constant, and at any given time, p is the same for all mass elements except those very close to the shock, hence

$$\rho \sim p_s^{-1/\gamma} \tag{3.6}$$

($\sim$ means proportional to).

If we now introduce the abbreviation

$$m = r^3 \tag{3.7}$$

which is proportional to the mass inside the mass element considered, and if we use (3.2), we find that at any given time

21

$$\rho \sim m^{1/\gamma} \tag{3.8}$$

The radius R is given by

$$R^3 = \int \frac{dm}{\rho} \sim \int \frac{dm}{m^{1/\gamma}} = m^{\frac{\gamma - 1}{\gamma}} - \text{const.} \tag{3.9}$$

We shall set the constant equal to zero which amounts to the (incorrect) assumption that (3.8) holds down to m = 0. Actually, the isothermal sphere gives the constant a finite, positive value.

To find the temperature distribution, we note that the enthalpy

$$H = \frac{\gamma'}{\gamma' - 1} \frac{p}{\rho} \tag{3.10}$$

We are using the enthalpy rather than the internal energy because the interior of the shock is at constant pressure, not constant density. The thermodynamic equation for H is

$$T \, dS = dH - v \, dp \tag{3.11}$$

At given pressure, i.e., given time, (3.8) to (3.10) give

$$H \sim \rho^{-1} \sim m^{-1/\gamma} \sim R^{-3/(\gamma-1)} \tag{3.12}$$

22

Now the approximate relation between internal energy and temperature is given by Gilmore,[13] Fig. 5, viz.,*

$$E = 4.2_5 \times 10^{11} \left(\frac{\rho}{\rho_0}\right)^{-0.1} T'^{1.5} \text{ erg/gm} \qquad (3.13)$$

where T' is the temperature in units of 10^4 degrees.

Using $\rho = \frac{p}{E(\gamma'-1)}$ from (3.3) and setting $\gamma' = 1.18$, which is a reasonable average (see Table II) we may rewrite (3.13):

$$E = 7.0 \times 10^{11} p^{-1/9} T'^{5/3} \qquad (3.14)$$

where p is the pressure in bars. Since H is proportional to E, (3.12) and (3.14) give

$$T \sim H^{3/5} \sim R^{-1.8/(\gamma-1)} \equiv R^{-\alpha} \qquad (3.15)$$

Using $\gamma' - 1 = 0.18$, which is not far from the average of Table II,

---

*The thermodynamic relation

$$\left(\frac{\partial E}{\partial v}\right)_T = T \left(\frac{\partial p}{\partial T}\right)_v - p$$

leads to a relation between $\gamma - 1$ and the exponents in the relation

$$E = A\rho^{-x} T^y$$

namely,

$$x = (\gamma - 1)(y - 1)$$

Since we have chosen $\gamma = 1.18$ and $y = 1.5$ this relation gives $x = 0.09$. This is in sufficient agreement with $x = 0.1$ as used in (3.13).

$$T \sim R^{-10} \qquad\qquad (3.16)$$

The numerical calculations of Brode[8] are in good agreement with this at the relevant times, from about 0.05 to 0.5 second.

It will be noted that (3.16) was obtained without integration of the hydrodynamic equations; it follows simply from the equation of state. The weakest assumptions are (1) the relation between E and T, (3.13), and (2) the neglect of the constant in (3.9). But in any case, T will be a very high power of R.

c. Mean Free Path and Radiating Temperature

The emission of radiation from a sphere of variable temperature is governed by the absorption coefficient. For visible light, the absorption coefficient increases rapidly with temperature.[16] For any given wave length, the emission will then come from a layer which is one optical mean free path inside the hot material.*

---

*Actually the maximum emission comes from deeper inside the fireball. To see this we compute the emission normal to the surface, $J = \int dr \mathcal{E}(R) e^{-D(R)} dR$ where $\mathcal{E} = \dfrac{2h\nu^3}{c^2 \ell} e^{-h\nu/kT}$ is the emissivity, and the remaining notation is as in the text (below). The integrand has a maximum at $R^*/\ell^* = n\alpha + \alpha h\nu/kT^*$. The optical depth at the maximum is $D^* = D(R^*) = \dfrac{n\alpha + \alpha h\nu/kT^*}{n\alpha - 1}$ which is about 2, rather than 1 in the blue. By steepest descents and with occasional use of $1/n\alpha = 0$ it turns out that $J = \dfrac{\sqrt{2\pi}}{e} \sqrt{1 + \dfrac{h\nu}{kT^*}} \, B(\nu, T^*)$, greater by about a factor 2 than the J used in the text.

Assume that the mean free path is

$$\ell = \ell_1 \, T'^{-n} \tag{3.17}$$

where the exponent n and the coefficient ℓ_1 depend on the wave length. Then the optical depth for a given R is

$$D(R) = \int_R^\infty \frac{dR'}{\ell(R')} \tag{3.18}$$

Using (3.15) and (3.17),

$$D(R) = \frac{1}{\ell(R)} \int_R^\infty \left(\frac{T(R')}{T(R)}\right)^n dR'$$

$$= \frac{1}{\ell(R)} \int_R^\infty \left(\frac{R}{R'}\right)^{n\alpha} dR'$$

$$= \frac{R}{(n\alpha - 1)\, \ell(R)} \tag{3.19}$$

A typical value of n is 5 [cf. (5.52)], and α is 10 or somewhat larger. Thus to make

$$D(R) = 1 \tag{3.20}$$

we need

25

$$\ell(R) \approx \frac{1}{50} R \qquad\qquad (3.21)$$

Since the interesting values of R are of the order of a few hundred meters, the emitting layer will be defined by the fact that the mean free path is about 5 to 10 meters.

Equations (3.18) to (3.21) hold for emission in the exactly radial direction. At an angle θ with the radius we get instead

$$\ell(R,\theta) = \frac{\ell(R)}{\cos \theta} \qquad\qquad (3.22)$$

The apparent temperature of the emitting layer is then, according to (3.17),

$$T(R,\theta) = T(R,0) \ (\cos \theta)^{1/n} \qquad\qquad (3.23)$$

where T(R,0) is the emission temperature for forward emission. The intensity of emission is a known (Planck) function of the wave length and the temperature. Since the apparent temperature decreases (though slowly) with θ, according to (3.23) there will be limb darkening. On the many photographs of atomic explosions, it should be possible to observe this limb darkening and thus check the value of n.

The relation (3.17) needs to hold only in the neighborhood of the value (3.21) of ℓ and is therefore quite general as long as ℓ decreases with increasing temperature. The exponent n should be determined at constant pressure. For certain wave lengths, especially in the ultra-

violet, (3.17) is not valid; these wave lengths are strongly absorbed by cold or cool air (Sec. 4c). For example, at $\rho = \rho_0$ and $T = 2000°$, the mean free path is less than 1 meter for all light[16] of $h\nu > 4.7$ ev ($\lambda < 0.26$ μ). Since the emission of light of such short wave length from such cool air is negligible, the fireball will not emit such radiation at all.

A detailed discussion of the absorption coefficient in the visible will be given in Sec. 4b. As can be seen from the tables of Meyerott et al.[16] and from our Table VI, for a density $\rho = \rho_0$ the mean free path is of the order of 5 meters at about $6000°$. This corresponds to a pressure[13] of about 25 bars. For $\rho = 0.1\rho_0$ the requisite mean free path of a few meters is obtained for about $10,000°$, with $p \approx 7$ bars. Thus for a relatively modest decrease in pressure, the effective temperature of radiation increases from 6000 to $10,000°$, corresponding to a very substantial increase in radiation intensity. This is the mechanism of the increase in radiation toward the second maximum. A more detailed discussion will be given in Sec. 5f.

d. Energy Supply

As long as the radiating temperature is low, not much energy will be emitted as radiation, and this emission will only slightly modify the cooling of the material due to adiabatic expansion. However, when the radiating temperature increases, the radiation cooling will exceed the adiabatic cooling to an increasing extent. It then becomes necessary to supply energy from the interior to the radiating surface.

Most of the radiation comes from a thickness of one optical mean free path near the radius at which (3.21) is satisfied. Let J be the radiation emitted per unit area per second (which will be of the order of the black body radiation; see below and Sec. 4c); then the loss of enthalpy due to radiation, per gram per second, will be

$$- \left(\frac{\partial H}{\partial t} \right)_{rad} = \frac{J}{\ell \rho} \tag{3.24}$$

Adiabatic expansion, according to (3.11), will give an enthalpy change

$$\left(\frac{\partial H}{\partial t} \right)_{adi} = \frac{1}{\rho} \frac{\partial p}{\partial t} \tag{3.25}$$

As long as the shock is strong, i.e., as long as p is large compared to the ambient pressure p_1, the pressure behaves as

$$p \sim t^{-1.2} \tag{3.26}$$

where t is the time from the explosion; therefore,

$$- \left(\frac{\partial H}{\partial t} \right)_{adi} = \frac{1.2}{\rho} \frac{p}{t} \tag{3.27}$$

The radiation will be a relatively small perturbation as long as (3.24) is smaller than (3.27). This will stop being the case when

$$\frac{J}{\ell} = 1.2 \frac{p}{t} \tag{3.28}$$

Now using (3.21) this gives

$$\frac{1.2}{50} \, p \, \frac{R}{t} = J \qquad\qquad (3.29)$$

Because of the steep dependence of temperature on R, (3.16), the radiating surface R will be close to the shock front R_s. Now the Hugoniot relations state that for γ close to 1

$$\dot{R}_s = \left(\frac{2p}{\rho_1}\right)^{1/2} \qquad\qquad (3.30)$$

where ρ_1 is the ambient density and $p_s = 2p$, the shock pressure. Furthermore, for the strong shock case,

$$R_s \sim t^{0.4}$$

$$\frac{R_s}{t} = 2.5 \, \dot{R}_s \qquad\qquad (3.31)$$

Inserting into (3.29),

$$0.06 \, \sqrt{2} \; p^{3/2} = J \, \rho_1^{1/2} \qquad\qquad (3.32)$$

The black body radiation at temperature $10^4 \, T'$ is

$$J_0 = 5.7 \times 10^{11} \, T'^4 \; erg/cm^2 \; sec \qquad\qquad (3.33)$$

Actually, only the radiation up to about $h\nu_0 = 2.75$ ev can be emitted to large distances because the absorption is too great for radiation of

29

higher frequency (above, and Sec. 4c). The fraction of the black body spectrum which can be emitted is given, in sufficient approximation, by

$$\mathcal{E} = \frac{1}{6} \int_0^{u_0} u^3 \, du \, e^{-u} = 1 - e^{-u_0} \left(1 + u_0 + \frac{1}{2} u_0^2 + \frac{1}{6} u_0^3 \right) \qquad (3.34)$$

where

$$u_0 = \frac{h\nu_0}{kT} \qquad (3.35)$$

For $T = 8000^\circ$, we have $u_0 = 4$ and the effective emissivity is then

$$\mathcal{E}(4) = 0.57 \qquad (3.36)$$

In (3.34) we have neglected the fact that the infrared, below about 1/2 ev, also cannot be emitted (Sec. 4a), and have approximated $(e^u - 1)^{-1}$ in the Planck spectrum by e^{-u}; both corrections are small. $T_0 = 8000^\circ$ has been chosen as a reasonable average temperature (see Sec. 5). Near this temperature, $\mathcal{E}$ varies about as $T^{-1.5}$, so that the actual radiation to large distances is about

$$J = 5.7 \times 10^{11} \, T_0'^4 \, \mathcal{E}(4) \left(\frac{T'}{T_0'} \right)^{2.5}$$

$$= 2.3 \times 10^{11} \, T'^{2.5} \qquad (3.37)$$

Solving (3.32) for p, with $\rho_0 = 1.29 \times 10^{-3}$ (normal air density) gives

$$p = 20 \left(\frac{\rho_1}{\rho_0}\right)^{1/3} T'^{5/3} \text{ bar} \qquad (3.38)$$

For $\rho_1 = \rho_0$, $T' = 0.8$, this is 14 bars.

At higher temperature ($T' > 1$), the ultraviolet can be transported as easily as the visible although it will not escape to large distances (Sec. 4c). Then it is reasonable to use the full black body radiation (3.33) for the emission. Inserting this into (3.32) gives

$$p = 40 \left(\frac{\rho_1}{\rho_0}\right)^{1/3} T'^{8/3} \qquad (3.39)$$

For $\rho_1 = \rho_0$, $T' = 1.0$, this is 40 bars.

Thus for p greater than 14 to 40 bars, the radiation is only a fraction of the adiabatic cooling, for lower pressure radiation cooling is more important. At the lower pressures then, energy must be supplied from the inside to maintain the radiation. This gives rise to a "cooling wave" moving inwards as will be discussed in Sec. 5.

It is interesting that the condition (3.38) refers to the pressure alone. Neither the local density nor the equation of state enters. The opacity of air enters only insofar as it determines the radiating temperature T' through the condition (3.21).

A more accurate expression for the limiting pressure will be derived in Sec. 5e. It will turn out to be considerably lower, about 5 bars.

4. ABSORPTION COEFFICIENTS

a. Infrared

The main absorption in the infrared is due to free-free electron transitions. These are treated incorrectly in the paper by Meyerott et al.,[16] in which it is assumed that such transitions occur only in the field of ions. At the important temperatures of 8000° or less, the degree of ionization is 10^{-3} or less. Therefore, the free-free transitions in the field of neutral atoms and molecules are much more important than those in the field of ions, even though each individual atom contributes far less than each ion.

The effectiveness of neutrals in inducing free-free transitions has been measured and interpreted by Taylor and Kivel[18] at the Avco-Everett laboratory. As compared to one ion, the effectiveness of the most important neutral species is

N_2: $2.2 \pm 0.3 \times 10^{-2}$

N: $0.9 \pm 0.4 \times 10^{-2}$

O: $0.2 \pm 0.3 \times 10^{-2}$

Thus nitrogen gives about the same contribution whether molecular or atomic, and the contribution of oxygen is very small. As a result, one atom of air is equivalent to about $\alpha = 0.8 \times 10^{-2}$ ion (of unit charge).

The free-free absorption coefficient in cm^{-1} is then

$$\mu_{ff} = 0.87 \times 10^3 \alpha T'^{-1/2} \left(\frac{\rho}{\rho_0}\right)^2 (e^-)(h\nu)^{-3}$$

$$= 7.0\, T'^{-1/2} \left(\frac{\rho}{\rho_0}\right)^2 (e^-)(h\nu)^{-3} \qquad (4.1)$$

where e^- is the number of electrons per air atom, the quantity tabulated in Gilmore,[13] and $h\nu$ is the quantum energy in ev. Table III gives some numbers for $h\nu = 1$ ev, four temperatures and three densities. At 8000°, the free-free absorption is substantial, at lower temperatures negligible. At $12,000^\circ$ the transitions are mostly in the field of ions, i.e., Meyerott's numbers need only slight correction, and the absorption is large.

Table III. Free-Free Absorption Coefficients (cm^{-1})
for $h\nu = 1$ ev

T	$\rho/\rho_0 = 1$	0.1	0.01
4,000	6.8^{-6}	1.9^{-7}	4.1^{-9}
6,000	5.5^{-4}	1.05^{-5}	1.9^{-7}
8,000	4.1^{-3}	8.7^{-5}	2.4^{-6}
12,000	2.1^{-1}	1.50^{-2}	1.12^{-3}

Note: for each value, the power of 10 is indicated by a superscript.

Another cause of absorption in the infrared is the vibrational bands of NO, which have an oscillator strength of about[24] 10^{-5} and $h\nu = 1/4$ ev. The resulting absorption coefficient is about

$$\mu_{NO} = 0.2 \frac{\rho}{\rho_0} (NO) \tag{4.2}$$

where (NO) is the number of NO molecules per air atom. This is a few percent at $\rho/\rho_0 = 1$ and $T = 4000$ to 8000°, giving $\mu = 2 \times 10^{-3}$ to 10^{-2} cm^{-1}. While this is of the order of magnitude relevant for emission,

(3.21), it is small compared to the free-free absorption at this low frequency, except at $T < 5000^{\circ}$. Its main effect is therefore to lower the radiating temperature in the infrared somewhat.

Since the free-free transitions are the main cause of infrared absorption, the electron density governs the temperature and density dependence. For $\rho/\rho_0 \geq 10^{-1}$ and $T \leq 8000^{\circ}$, the main species of positive ions is NO^{+}. The ionization energy of NO is 9.25 ev; therefore, the electron density is roughly proportional to

$$\rho^{3/2} \exp\left(-\frac{9.25 \text{ ev}}{2 \text{ kT}}\right) \tag{4.3}$$

From 6000 to 8000°, this gives a factor of about 10 in the electron density, in accord with Gilmore's tables. Near 8000°, we may write approximately

$$\mu_{ff} \sim (e^{-}) \sim \rho^{3/2} T^{7} \tag{4.4}$$

Writing $\rho \sim pT^{-1.5}$, this gives

$$\mu_{ff} \sim p^{3/2} T^{5} \tag{4.5}$$

The temperature dependence of the absorption in the visible will turn out about the same.

b. Visible

In the visible and for temperatures below about $10,000^{\circ}$, the main

causes of absorption are the molecular bands of

N_2 (first positive) from about 1 to 2-1/4 ev

N_2^+ (first negative)   "   "   2-1/2 to 3-3/4 ev

NO (β bands)   "   "   2-1/2 to 6 ev

and the continuous absorption due to O^- photodetachment from about 1-1/2 ev up. The N_2 second positive, and O_2 Schumann-Runge, although they contribute, are usually weaker than the combination of N_2^+ first negative and NO and cover the same region of the spectrum (or less). O^- photodetachment is mostly important at the higher density, $\rho/\rho_0 = 1$.

There is commonly a "window" of low absorption below 1 ev, between free-free absorption and $N_2(1^+)$, and another at about 2-1/2 ev, between N_2 and the other bands (Table IV). The latter window is filled in by O^- photodetachment. At higher temperature, such as $12,000^\circ$, the photoelectric effect on N and O becomes important and the molecular bands almost disappear; the absorption coefficient is then almost uniform over the entire spectrum.

The table by Meyerott et al. should be consulted for details. Apart from the free-free transitions, this table seems to be in error on the $N_2(1^+)$ absorption at 8000°, which should be increased by a factor of 4. With these corrections, Table IV gives the absorption coefficients at 8000° for a few frequencies and densities, mentioning in each case only the most important species of absorbers. For $\rho/\rho_0 = 0.1$ and 0.01, the contribution of NO and O_2 in the wave length region considered is negligible. The windows at 1 and above 2 ev are noticeable in the table; beyond 3 ev there is a rapid increase in absorption.

35

Table IV. Contributions to Absorption Coefficients at $8000°$

$h\nu$ (ev)	5/8	1-1/8	1-5/8	2-1/8	2-5/8	3-1/8
$\rho/\rho_0 = 1$						
ff	1.7^{-2}	0.3^{-2}	0.10^{-2}	0.04^{-2}	0.02^{-2}	0.01^{-2}
N_2		1.1^{-2}	2.1^{-2}	0.84^{-2}	0.04^{-2}	0.56^{-2}
O^-			0.21^{-2}	0.28^{-2}	0.31^{-2}	0.32^{-2}
NO, N_2^+, O_2					0.31^{-2}	2.2^{-2}
Total	1.7^{-2}	1.4^{-2}	2.4^{-2}	1.16^{-2}	0.68^{-2}	3.1^{-2}
$\rho/\rho_0 = 0.1$						
ff	0.36^{-3}	0.06^{-3}	0.02^{-3}	0.01^{-3}		
N_2		0.61^{-3}	1.12^{-3}	0.46^{-3}	0.02^{-3}	0.30^{-3}
O^-			0.05^{-3}	0.06^{-3}	0.07^{-3}	0.07^{-3}
N_2^+					0.55^{-3}	4.2^{-3}
Total	0.36^{-3}	0.67^{-3}	1.2^{-3}	0.53^{-3}	0.64^{-3}	4.6^{-3}
$\rho/\rho_0 = 0.01$						
ff	1.0^{-5}	0.17^{-5}	0.05^{-5}	0.02^{-5}	0.01^{-5}	0.01^{-5}
N_2		1.39^{-5}	2.6^{-5}	1.03^{-5}	0.05^{-5}	
O^-			0.13^{-5}	0.17^{-5}	0.2^{-5}	0.2^{-5}
N_2^+				0.03^{-5}	4.4^{-5}	34^{-5}
Total	1.0^{-5}	1.6^{-5}	2.8^{-5}	1.25^{-5}	4.7^{-5}	34^{-5}

The concentration of all the absorbing species depends strongly on temperature: The N_2 first positive absorption starts from the electronic level A, which has an excitation energy of 5.7 ev; NO itself requires high temperature for its formation; and N_2^+ and O^- are ions whose concentration behaves like the electron concentration, discussed above in Sec. 4a. Therefore, the absorption depends strongly on temperature. N_2 first positive is the most important absorber, and its temperature dependence (relative to the ground state of N_2) is about

$$ \exp\left(-\frac{5.7 \text{ ev}}{kT}\right) \tag{4.6} $$

The concentration of N_2 up to 6000° is nearly independent of density, but at 8000° it is about proportional to $\rho^{1/2}$ (per air atom) so that near 8000°

$$ \mu_{N_2} \sim \rho^{3/2} T^8 \tag{4.7} $$

which is nearly the same dependence as derived in (4.4) for the free-free transitions. In terms of pressure we get

$$ \mu_{N_2} \sim p^{3/2} T^6 \tag{4.8} $$

Table V gives the absorption coefficients for four temperatures, three densities, and six wave lengths. In the visible (1-1/8 to 2-5/8 ev) the strong increase in absorption with temperature is evident, a factor

Table V. Absorption Coefficients in Visible (cm^{-1})

ρ/ρ_0	T	$h\nu = 5/8$	1-1/8	1-5/8	2-1/8	2-5/8	3-1/8
1	4,000	27^{-6}	7.5^{-6}	5.3^{-6}	1.5^{-6}	52^{-6}	8900^{-6}
	6,000	2.3^{-3}	1.10^{-3}	2.1^{-3}	1.53^{-3}	1.66^{-3}	11^{-3}
	8,000	1.7^{-2}	1.4^{-2}	2.4^{-2}	1.16^{-2}	0.68^{-2}	3.1^{-2}
0.1	4,000	7.8^{-7}	4.2^{-7}	4.2^{-7}	1.05^{-7}	35^{-7}	4100^{-7}
	6,000	4.3^{-5}	7.6^{-5}	13.7^{-5}	7.5^{-5}	4.8^{-5}	26^{-5}
	8,000	3.6^{-4}	6.7^{-4}	12^{-4}	5.3^{-4}	6.4^{-4}	46^{-4}
	12,000	6.1^{-2}	1.2^{-2}	1.5^{-2}	0.84^{-2}	0.85^{-2}	1.42^{-2}
0.01	4,000	1.7^{-8}	3.3^{-8}	4.0^{-8}	0.90^{-8}	16^{-8}	900^{-8}
	6,000	0.8^{-6}	5.7^{-6}	10.3^{-6}	4.8^{-6}	2.8^{-6}	25^{-6}
	8,000	1.0^{-5}	1.6^{-5}	2.8^{-5}	1.25^{-5}	4.7^{-5}	34^{-5}
	12,000	4.6^{-3}	0.48^{-3}	1.30^{-3}	0.72^{-3}	0.68^{-3}	0.91^{-3}

of about 200 from 4000 to 6000°, about 10 from 6000 to 8000° except for the lowest density, and 10 to 50 from 8000 to $12,000^{\circ}$. In most cases, the dependence on wave length is slight until the rapid increase of absorption in the ultraviolet which sets in at about 2.5 ev for 4000°, 3 ev at 6000 and 8000°, and not at all at $12,000^{\circ}$. The especially strong increase for 4000° is due to the Schumann-Runge bands, which are not very sensitive to temperature[*,†] (see Sec. 4c).

In Sec. 5d we shall need the mean free path in gm/cm^2, suitably averaged over the "transparent" region. From Table V it appears that a reasonable estimate of this region is from $h\nu = 1/2$ to 2-3/4 ev. We have averaged ρ/μ as calculated from Table V, with the weighting factor

$$u^3 e^{-u}, \qquad u = \frac{k \times 8000^{\circ}}{h\nu} \tag{4.9}$$

which does not vary much (from 0.84 to 1.33) between 1-1/8 and 2-5/8 ev. The result is given in Table VI.

---

[*]After completion of this paper, I received new absorption coefficients by F. R. Gilmore, cf. ref. 23. Aside from including the absorption by NO_2 (see Sec. 4a), Gilmore includes the free-free absorption in the field of neutrals, based on ref. 18, and also new data on f numbers for the important bands.[24] The most important change is a reduction in the f number of the N_2 first positive system from 0.02 to 0.0028, which will substantially reduce the absorption in the visible. Unfortunately, this will further raise the theoretical radiating temperature (Sec. 5d), which is already higher than observed.

[†]Some recent Avco-Everett experiments may indicate that the free-free electron transitions in the field of the N atom are enhanced in the visible as compared to the infrared. This may compensate to some extent for the reduction of the N_2 first positive bands (see footnote above).

Table VI. Average Mean Free Paths (gm/cm^2)

T	$\rho/\rho_0 = 1$	0.1	0.01
6,000	0.86	1.34	3.15
8,000	0.105	0.20	0.76
12,000		1.25^{-2}	1.82^{-2}

A fair approximation to Table VI is

$$\frac{\rho}{\mu} = 2.7 \times 10^{-2} \left(\frac{\rho}{\rho_0}\right)^{-0.3} T'^{-7} \tag{4.10}$$

Gilmore's equation of state can be approximated near $T' = 1$, $\rho/\rho_0 = 0.1$ by

$$p = 55 \left(\frac{\rho}{\rho_0}\right)^{0.9} T'^{3/2} \tag{4.11}$$

Using this in (4.10) gives

$$\frac{\rho}{\mu} = 0.10 \, p^{-1/3} \, T'^{-6.5} \, gm/cm^2 \tag{4.12}$$

c. Ultraviolet

The absorption in the ultraviolet is generally high at all temperatures. At low temperatures, the absorption is mainly due to the Schumann-Runge bands; at higher temperature (8000°) these are replaced by NO β and γ, and at high temperature $(12,000^\circ)$ by photoelectric absorption in O^-,

N, and O. The Schumann-Runge bands start from the electronic ground state of O_2, hence are available at low T; at higher T, the spectral region of strong absorption spreads due to excitation of vibrational states; but at still higher T, oxygen dissociates and therefore the bands die out (at 8000°, they contribute less than 10% of the absorption). The photoelectric absorption in N and O requires not only the presence of these atoms but also their electronic excitation,[*] and therefore does not become important until about $10,000^\circ$.

Table VII gives, for density $\rho = 0.1\rho_0$, the spectral regions of strong absorption. In accord with Sec. 3b, we define this by $\mu > 10^{-3}$ (mean free path less than 10 meters) or $\mu > 10^{-2}$ ($\ell < 1$ meter). The table shows that strong absorption covers a particularly wide spectral region at 4000°, shrinking substantially at 6000°. Very strong absorption, $\mu > 10^{-2}$ cm^{-1}, occurs in quite a large spectral region for T = 4000° but shrinks to practically nothing at 6000° and to nothing at 8000°. At $12,000^\circ$, very strong absorption occurs again but is now in the visible.

The strong absorption in the ultraviolet ($h\nu > 3.5$ ev) means first of all that the UV is not emitted to large distances and can therefore not be observed; e.g., at T = 4000° and $h\nu = 3.5$ ev, we have

$$u = \frac{h\nu}{kT} = 10$$

---

[*]We should also add the photoelectric absorption from excited states of NO, which should be especially noticeable at 8000°.

The fraction of the Planck spectrum beyond u = 10 is only about 1%, so that emission of these frequencies is negligible.

Table VII. Ultraviolet Absorption: Spectral Regions (hν in ev) with Large Absorption as a Function of Temperature for $\rho = 0.1\rho_0$

T	$\mu > 10^{-3}$ cm^{-1}	$\mu > 10^{-2}$ cm^{-1}
2,000	4.7 - 7.2	5.5 - 7.2
3,000	3.9 - 7.2	4.7 - 7.2
4,000	3.5 - 7.2	4.6 - 7.2
6,000	4.0 - 7.1	5.8 - 6.0
8,000	2.7 - 6.3	None
12,000	All	2.7 - 3.5

The ultraviolet can, however, be transported quite easily at 8000° and even more easily at 12,000° if there is a temperature gradient. Such a gradient is always available, whether we have adiabatic conditions (Secs. 3b, 5f) or a strong cooling wave (Sec. 5d). Therefore, there will be a flow of ultraviolet radiation at the radiating temperature, defined in Sec. 5, which will be shown (Secs. 5d, 5f) to be about 10,000° or slightly less. To calculate this flow, we should determine the temperature gradient from considerations such as Sec. 5d or 5f, and then insert this into the radiation flow equation. This is similar to (5.3) except that only the ultraviolet contribution to the flow should be taken into account.

When this is done in a case of constant (frequency-independent) absorption coefficient, the ultraviolet transport will be related to the visible radiation transport as the respective intensities in the Planck spectrum. This condition seems to be nearly fulfilled at 12,000°. At 8000°, the absorption in the near ultraviolet (2.75 to 4.2 ev) is about three times that in the visible; then the UV transport will be one-third of that corresponding to the Planck intensity. Since the radiating temperature near the second radiation maximum is between 8000 to 10,000°, the actual UV transport will be between one-third and the full Planck value, relative to the visible radiation. According to (3.36), the UV contains about 43% of the Planck intensity at 8000°; hence the total radiation transport at this temperature is about

$$57 + 1/3 \times 43 = 71\%$$

of the black body radiation. At 12,000° we get the full black body value. For simplicity we have assumed the full black body radiation in Sec. 5, even though the UV is not emitted to large distances. But this problem could, and should, be treated more accurately.

Having discussed the influence of the UV on the total radiation flow, we now examine what happens to the UV radiation after it has gone through the "radiating layer," i.e., the layer which emits the visible light to large distances. The very near ultraviolet, 2.75 to 3.5 ev, will be partially absorbed at 4000 to 6000°, especially if the layer of matter at these intermediate temperatures becomes thick, 0.3 to 0.5 gm/cm^2 or so.

The UV beyond 3.5 ev will be strongly absorbed at 4000°. Thus the layers of air at intermediate temperatures get additional heat which counteracts and may even exceed the adiabatic cooling. This will tend to increase the thickness of the medium-temperature layer. This in turn will (moderately) lower the radiating temperature, but three-dimensional effects act the opposite way (Sec. 6).

5. THE COOLING WAVE

a. Theory of Zel'dovich et al.

Zel'dovich, Kompaneets, and Raizer [10] (quoted as Z) have considered the loss of radiation by hot material when the absorption coefficient for the radiation increases monotonically with temperature. They have shown that in this case a cooling wave proceeds into the hot material from the outside. This is to say, the cool temperature outside gradually eats its way into the hot material, while the material in the center remains unaffected and merely expands adiabatically.

For simplicity, Zel'dovich et al. consider a one-dimensional case. They further assume that the specific heat is constant and express their theory in terms of the temperature. This is not necessary; we shall merely assume that both the enthalpy H and the absorption coefficient for radiation are arbitrary but monotonically increasing functions of the temperature. Like Z, we shall assume, in this subsection only, that the radiation transport can be described by an opacity (Rosseland mean) rather than considering each wave length separately.

44

The fundamental statement of Z is that the cooling wave keeps its shape, i.e., that the enthalpy (and other functions of the temperature) is given by

$$H = H(x + ut) \qquad (5.1)$$

Here t is the time, x is the Lagrangian coordinate, and u is the Lagrangian velocity of the cooling wave. We have written x + ut so that the cooling wave proceeds towards smaller x, i.e., inwards. H is, of course, a decreasing function of x + ut. The Lagrangian coordinate is best measured in gm/cm^2 and is defined by

$$x = \int \rho \, dX \qquad (5.2)$$

where X is the geometrical (Eulerian) coordinate. For given pressure p, the density ρ is a function of H so that X(x) can be calculated from (5.2). The Lagrangian velocity u, measured in gm/cm^2 sec, is a constant.

For any given H, we know the temperature T, hence the opacity K and the radiation flow

$$J = -\frac{4}{3} \frac{a}{K(T)} \frac{\partial(T^4)}{\partial x} \qquad (5.3)$$

where a is the Stefan-Boltzmann constant,

$$a = 5.7 \times 10^{-5} \ erg/cm^2 \ sec \ deg^4$$

The equation of continuity is

$$\frac{\partial H}{\partial t} = -\frac{\partial J}{\partial x} \qquad (5.4)$$

The energy in radiation has been neglected, which is justified in all practical cases. Using (5.1), (5.4) can be integrated over x to give

$$uH + J = C \qquad (5.5)$$

where C is a constant. This is the fundamental result of Z.

If the opacity increases monotonically with H, then in the interior J will be very nearly zero, and therefore

$$C = uH_0 \qquad (5.6)$$

where H_0 is the enthalpy in the undisturbed interior, hot region. Equation (5.5) becomes

$$J = u(H_0 - H) \qquad (5.7)$$

and using (5.3)

$$dx = -\frac{4}{3} a \frac{d(T^4)}{K(T,p)(H_0 - H)} \qquad (5.8)$$

which can be integrated to give $x(T)$, since $H(T)$ and $K(T,p)$ are known functions. We have put in evidence the fact that K depends on pressure in addition to T. Over most of the range of T, $K(T)$ is the most rapidly

varying (increasing) function of T and the variation of H_0 - H is less important; therefore, T(x) becomes steeper as T increases; but when H gets very close to H_0, the most rapidly varying function in (5.8) is H_0 - H, and H approaches H_0 exponentially as $e^{\alpha x}$ for small x. The qualitative behavior of T(x) is shown in Fig. 1, in accord with Z. To obtain this shape it is essential that K(T) increase much faster than T^3.
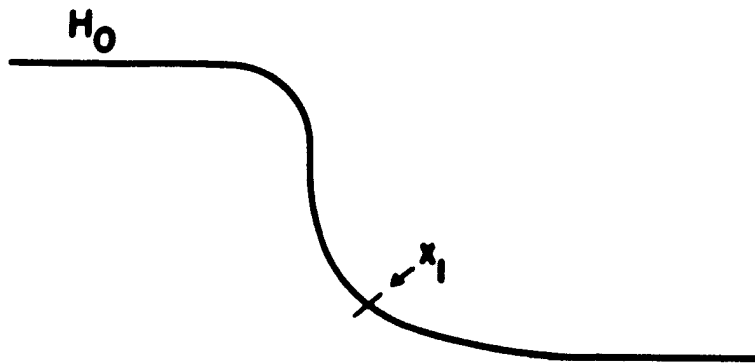

Fig. 1. Temperature distribution in cooling wave.

On the outside, we finally come to a point x_1 where only one optical mean free path is outside x_1. From this point we get black body emission, i.e., (5.3) is replaced by

$$J(x_1) \equiv J_1 = aT_1^4 \qquad (5.9)$$

Using this in (5.7) we find

$$u = \frac{J_1}{H_0 - H(T_1)} \tag{5.10}$$

To determine u we therefore have to proceed as follows:

1. Find the temperature T_1 at which the opacity $K(T_1)$ is such that there is one optical mean free path outside x_1, i.e.,

$$\int_0^{T_1} K(T) \, dx(T) = 1 \tag{5.11}$$

For this purpose we must know, of course, the temperature distribution $T(x)$ for $T < T_1$.

2. Determine $J(T_1)$ from (5.9) and $H(T_1)$ from the equation of state.

Knowing the internal enthalpy H_0 then gives u from (5.10). Note that u is the Lagrangian velocity of the cooling wave. It has the correct dimension.

To solve problem 1, Z assume that the material which has gone through the cooling wave will expand adiabatically. We shall find that this is a reasonable assumption in most conditions (Sec. 5d) but that at early times (Sec. 5f) and in certain late stages other considerations apply (Sec. 6b).

b. Inside Structure of Fireball, Blocking Layer

In early stages (Stage B I), just after the shock wave is formed, the isothermal sphere expands, by radiation diffusion, into the material which has been heated by shock. This process, which will be treated in a subsequent report, depends on the temperature and temperature gradient

in the isothermal sphere. For its occurrence it is important that the opacity actually _decreases_ with increasing T at higher temperature. Many calculations of K(T) in this temperature region have been made. Curves have been compiled, especially by Gilmore,[21] and revised as more information has become available. The most recent and most extensive calculation, to my knowledge, is by Stuart and Pyatt.[22]

All calculations agree that $T^3/K(T)$, which is the important quantity according to (5.3), has a pronounced minimum at about $T' = 2$, $T = 20,000°$. (The temperature of the minimum increases slightly with increasing density.) Molecules are no longer present at these temperatures, and absorption is mainly by bound-free electron transitions in atoms and atomic ions, with some contribution from broadened atomic lines (bound-bound transitions) whose calculation is the most difficult. Radiation transport, then, is most difficult around $T_b = 20,000°$, and temperatures around T_b constitute an effective blocking layer for radiation.

Until about 0.5 second, the central temperature of a 1-megaton sea level explosion is greater than T_b, according to the calculations of Brode.[8] Radiation flow can then be considered as taking place separately in an _interior_ and an _exterior_ region. The interior flow is determined by the central temperature T_c, and this flow generally decreases with time because T_c decreases and with it the quantity T^3/K. The exterior flow is dominated by the cooling wave and increases with time because the decrease of density causes a decrease of opacity for any given T. The two flow regions are separated by a blocking layer in which the

49

temperature is around T_b, and in which the temperature distribution is essentially that originally established by shock and subsequent adiabatic expansion. It is to this condition that the temperature distribution (3.16), $T \sim R^{-10}$, refers.

The radiation flow through the blocking layer is

$$J_b = -\frac{4}{3} aT_b^4 \frac{\ell_b}{R_b} 4 \frac{d \log T}{d \log R} \qquad (5.12)$$

The mean free path for radiation in the blocking layer (at $18,000^\circ$) according to Gilmore[21] is about

$$\ell_b = 0.8 \left(\frac{\rho}{\rho_0}\right)^{-1.3} cm \qquad (5.13)$$

The radius R_b at which this temperature occurs, for a 1-megaton explosion at sea level, is $R_b = 300$ to 400 meters. Using $T \sim R^{-10}$, this gives

$$J_b = 7 \times 10^9 \left(\frac{\rho}{\rho_0}\right)^{-1.3} \qquad (5.14)$$

This is equivalent to black body emission at the effective temperature

$$T_{eff,b} = 3300 \left(\frac{\rho}{\rho_0}\right)^{-0.325} \qquad (5.15)$$

Using the equation of state at $18,000^\circ$,

$$\frac{\rho}{\rho_0} = \left(\frac{p}{150}\right)^{1.1} \qquad (5.16)$$

where p is in bars. Equation (5.15) becomes

$$T_{eff,b} = 20,000 \ p^{-0.36} \qquad (5.17)$$

The "blocking layer" will deserve its name only if the radiating temperature is higher than $T_{eff,b}$.

c. Velocity of Cooling Wave

The velocity of the cooling wave is given by (5.10), where H_0 is the enthalpy at the point to which the cooling wave has proceeded. If inside this point there is a noticeable flow of radiation, J_0, (5.10) should be generalized to

$$u = \frac{J_1 - J_0}{H_0 - H(T_1)} \qquad (5.18)$$

Usually, the main dependence on the internal conditions is through H_0, the effect of J_0 being less important.

As H_0 increases, i.e., as the wave progresses more into the interior, the velocity of the wave will decrease. The limit will be reached when the cooling wave penetrates the isothermal sphere; then H_0 is the enthalpy in that sphere and $J_0 = 0$. We now use the black body formula (3.33) for the emission of radiation at the radiating surface T_1, (3.14) for the

51

internal energy in the isothermal sphere of temperature T_c and $\gamma' = 1.15$ in that sphere; then (5.18) becomes

$$u_c = \frac{5.7 \times 10^{11} \, T_1'^4}{8.2 \times 10^{11} \, p^{-1/9} \, (T_c'^{5/3} - T_1'^{5/3})}$$

$$= 0.70 \, p^{1/9} \, \frac{T_1'^4}{T_c'^{5/3} - T_1'^{5/3}} \quad gm/cm^2 \ sec \qquad (5.19)$$

Typically, $p = 5$, $T_1' = 1$, $T_c' = 3$; then $u = 0.15 \, gm/cm^2$ sec. The expression (3.33) includes all the black body radiation. If only the radiation actually emitted to large distances is to be included (which is reasonable at lower temperatures, $T_1' < 0.8$) (3.37) should be used; then u will be smaller, $0.1 \, gm/cm^2$ sec or less.

Before the cooling wave reaches the isothermal sphere, H_0 is smaller. This is partly compensated by the fact that $J_0 > 0$. An interesting intermediate state is when the cooling wave has just reached the blocking layer. Then, using $T_b' = 1.8$ and (5.14),

$$u_b = \frac{J_1 - J_b}{H_b - H_1} \qquad (5.20)$$

$$= 0.70 \, p^{1/9} \, \frac{T_1'^4 - 16 \, p^{-1.44}}{2.7 - T_1'^{5/3}} \qquad (5.21)$$

Clearly this makes sense only if the subtracted term in the numerator is

smaller than the first term, i.e., when the pressure is sufficiently high. As the pressure decreases below about 10 bars, the blocking layer "opens up" and ceases to block the flow of radiation.

In the very beginning, when the cooling wave just starts, the top temperature of the cooling wave, T_0, is close to the radiating temperature T_1. Then (5.18) becomes

$$u_1 = - \left(\frac{dJ}{dH}\right)_{T_1} \tag{5.22}$$

If we use (5.12) for J, assume d log T/d log R and R to be constant, and use (3.14), then

$$u_1 \sim - \left(\frac{d(\ell T^4)}{T^{2/3} \, dT}\right)_{T_1} \tag{5.23}$$

For further discussion, see Sec. 5f.

As T increases, u decreases from (5.23) via (5.21) to (5.19). After the cooling wave has penetrated to the isothermal sphere, u is apt to increase again because T_c in the denominator of (5.19) will decrease due to adiabatic expansion of the isothermal sphere. Thus the velocity u is apt to be a minimum when the cooling wave has just reached the isothermal sphere.

The variation of u with time is not very great. Likewise, the shape of the cooling wave changes only slowly with time. The shape is obtained

by integrating (5.8); it depends on time because K is a (rather slowly variable) function of the pressure, and H_0 is a (slow) function of time. This justifies approximately the basic assumption (5.1) of Z: While the cooling wave does not preserve its shape exactly, it does so approximately.

The picture is then that at any given time t there are up to five regions behind the shock. In Fig. 2 the temperature is plotted schematically against the Lagrange coordinate r. Starting from the center, there is first the isothermal sphere (I in Fig. 2).
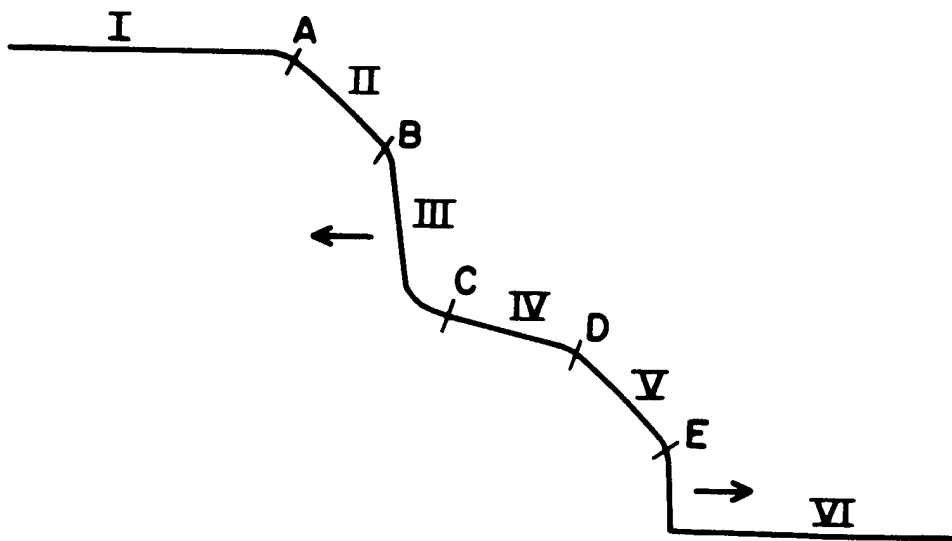

Fig. 2. Schematic temperature distribution. I, isothermal sphere; III, cooling wave; VI, undisturbed air; E, shock front. II, IV, and V are expanding adiabatically.

This may be followed by a region II in which the temperature distribution is essentially that established by adiabatic expansion behind the

shock, Eq. (3.15). Next comes the cooling wave III in which the temperature falls more steeply, according to (5.8). (At late times, region II is wiped out and III follows immediately upon I.) Region IV includes the material which has gone through the cooling wave, and now cools adiabatically; hence the temperature falls slowly with r (Sec. 5d). D is the material point from which the cooling wave started originally; region V, outside that point, is also expanding adiabatically, but from shock conditions; thus it is the continuation of region II. Finally region VI is the air not yet shocked. As time goes on, the cooling wave III moves inward, wiping out region II and then eating into region I. Region IV accordingly grows toward the inside, but its outer end D stays fixed. Region V expands into VI by shock.

We note once more that u is the velocity in Lagrange coordinates, and in gm/cm^2 sec. The problem is made somewhat more complicated by the three dimensions and the adiabatic expansion, cf. Sec. 6, but the principal features remain the same.

d. Adiabatic Expansion after Cooling. Radiating Temperature

When a given material element has gone through the cooling wave, it is left at the radiating temperature T_1. Thereafter, it will expand adiabatically. Equation (3.25) shows that for adiabatic expansion

$$\left(\frac{\partial H}{\partial t}\right)_{adi} = \frac{1}{\rho}\frac{\partial p}{\partial t} \tag{5.24}$$

or, using (3.10)

$$\frac{\partial \log H}{\partial t} = \frac{\gamma' - 1}{\gamma'} \frac{\partial \log p}{\partial t} \tag{5.25}$$

As long as the shock is strong, (3.26) holds and therefore

$$\frac{\partial \log H}{\partial \log t} = -1.2 \frac{\gamma' - 1}{\gamma'} \tag{5.26}$$

Gilmore's[13] Tables 11 and 15 show that for $T = 5000$ to 8000°, and $p = 1$ to 10 bars, γ' varies from about 1.13 to 1.20, so

$$\frac{\partial \log H}{\partial \log t} = -0.14 \text{ to } -0.20 \tag{5.27}$$

At late times, p no longer decreases as fast as $t^{-1.2}$, so H also decreases more slowly but (5.25) remains valid.

We use now the approximate equation of state (3.14) (together with $H = \gamma' E$) and find

$$T' \sim p^{1/15} H^{3/5}$$

$$\sim p^{\frac{1}{15} + \frac{3}{5} \frac{\gamma' - 1}{\gamma'}}$$

$$= p^\beta \tag{5.28}$$

with

$$\beta = \frac{2}{3} \frac{\gamma' - 0.9}{\gamma'}$$

$$= 0.136 \text{ to } 0.167 \tag{5.29}$$

56

using (5.25) and $\gamma' = 1.13$ to 1.20. A given material element which went through the cooling wave at temperature T'_m and pressure p_m will now (at pressure p) have the temperature

$$T' = T'_m \left(\frac{p}{p_m}\right)^\beta \tag{5.30}$$

If we assume T_m to be independent of time, then at a given time in the adiabatic region (IV of Fig. 2)

$$\frac{\partial \log T'}{\partial x} = -\beta \frac{\partial \log p_m}{\partial x} = \frac{\beta}{u} \frac{\partial \log p_m}{\partial t_m} \tag{5.31}$$

$$= -\frac{1.2\beta}{ut_m} = -\frac{0.8}{ut_m} \frac{\gamma' - 0.9}{\gamma'} \tag{5.32}$$

where t_m is the time at which the material element x was radiating. The last step in (5.31) assumes that the velocity of the radiation wave is constant but is valid whatever the time dependence of the pressure; (5.32) assumes $p \sim t^{-1.2}$, i.e., strong shock conditions. It should be noted that t in the relation $p \sim t^{-1.2}$, and therefore t_m in (5.32), is the total time since the nuclear explosion.

The velocity u of the cooling wave was calculated in Sec. 3c, (5.18), (5.19), etc. The condition for the radiating surface, now as in Sec. 3c, is that there be one optical mean free path outside it for "visible" light as defined in Sec. 4b. Since we now use material coordinates in gm/cm^2, we should use mean free paths in the same unit. Table VI and (4.10) and (4.12) give the required information. We write (4.12) in the form

$$\frac{\rho}{\mu} = Ap^{-1/3} \, T'^{-n} \tag{5.33}$$

with $A = 0.10 \ gm/cm^2$ and $n = 6.5$.

The optical depth is, according to (5.32) and (5.33)

$$D = \int_{x_1}^{\infty} \frac{dx}{\rho/\mu} = \left(-\frac{dx}{d \ln T'} \right) \frac{p^{1/3}}{A} \int_{0}^{T'_1} \frac{d \ln T'}{T'^{-n}} \tag{5.34}$$

$$= \frac{1}{n} \frac{ut}{0.8} \frac{\gamma'}{\gamma' - 0.9} \frac{p^{1/3} T_1'^{n}}{A} \tag{5.35}$$

Setting $D = 1$, $\gamma' = 1.15$, $A = 0.10$, and $n = 6.5$ gives

$$T_1'^{6.5} = \frac{0.11 \ gm/cm^2}{ut} p^{-1/3} \tag{5.36}$$

This is an explicit expression for the radiating temperature in terms of the velocity of the cooling wave. The latter depends in turn on the radiating temperature, increasing with $T_1'^{4}$, so that T_1' occurs altogether in the 10.5 power and thus can be determined very accurately.

Equation (5.36) can be further reduced by using the relation between pressure and time which is, for a strong shock, approximately

$$tp^{5/6} = 1.0 \ Y^{1/3} \left(\frac{\rho_1}{\rho_0} \right)^{1/2} \tag{5.37}$$

where t is in seconds, p in bars, and Y in megatons, and ρ_1 is the density of the ambient, undisturbed air. Then (5.36) becomes

$$uT_1^{'6.5} = 0.11 \, Y^{-1/3} \left(\frac{\rho_0}{\rho_1}\right)^{1/2} p^{1/2} \tag{5.38}$$

The right hand side of (5.38) gives the complete dependence on Y and ρ_1 since, in deriving (5.36), we have only used the opacity law (5.33) and the adiabatic cooling of air, (5.32), both of which are independent of the explosive yield Y and of the ambient density of the air.

Now insert u from (5.19); then we obtain

$$\frac{T_1^{'10.5}}{T_c^{'5/3} - T_1^{'5/3}} = 0.16 \, Y^{-1/3} \left(\frac{\rho_0}{\rho_1}\right)^{1/2} p^{7/18} \tag{5.39}$$

This equation gives the radiating temperature in terms of the central temperature T_c and of the quantities on the right hand side. The radiating temperature is proportional to a low power of the central temperature (about the 1/6 power); thus as the inside cools, the radiation decreases (see Sec. 5e for details). It also decreases slowly with time due to the pressure factor on the right hand side, $T_1' \sim p^{1/27}$. For given p and T_c, the radiation temperature is higher for lower yield, $T_1' \sim Y^{-0.032}$, and for higher altitude, $T_1' \sim \rho_1^{-1/21}$.

For sea level, for Y = 1, and for p = 5 bars (cf. Sec. 5e for this choice) Brode's calculations give $T_c' \approx 3.6$; then (5.39) yields $T_1' = 1.08$,

or a radiating temperature of 10,800°. This is a reasonable result, though appreciably higher than the temperatures usually observed. However, as we shall show in Secs. 5e and f, our calculation gives the maximum temperature reached, and is likely to be somewhat too high due to our approximations.

e. Beginning of Strong Cooling Wave

Equation (5.19) gives the inward speed of the cooling wave in gm/cm^2 sec. Precisely, this is the speed at which the point of temperature T_1 (radiating temperature) moves relative to the material, once the cooling wave is fully established. But even if there is no cooling wave, i.e., if we have simply adiabatic expansion behind the shock, a point of given temperature T_1 will move inward. This "adiabatic motion" is the minimum velocity which the point T_1 can have. Therefore, if the adiabatic speed is greater than (5.19), it will be the correct velocity. Of course, there will still be a cooling wave because this is needed to supply the energy for the radiation; this "weak cooling wave" will be described in Sec. 5g. But its inward motion, more accurately the velocity of its foot (point C in Fig. 2), will not be determined by the requirement of sufficient energy flow, (5.19), but by the "adiabatic speed" which we shall derive from (3.15). Region IV of Fig. 2 will now be absent. Thus, outside the cooling wave, at point C, region V will begin immediately, with the temperature distribution given by (3.15).

It is therefore important to determine the time t_a (and pressure p_a)

60

at which u of (5.19) becomes larger than the adiabatic speed of temperature T_1. Before this time t_a, we have a weak cooling wave. We call this Stage C I; afterwards, the cooling wave is strong, and the radiation is essentially described by the theory of Sec. 5d (Stage C II). To determine the point of separation p_a between these two stages is a refinement of the considerations of Sec. 3d.

The temperature in the adiabatically expanding material behind the shock is a function of time and position, given by hydrodynamics and equation of state. The inward motion of a point of given temperature relative to the material is given by

$$- \rho \frac{dr}{dt} = \frac{(\partial \log T/\partial t)_r}{(\partial \log T/\rho\, \partial R)_t} \tag{5.40}$$

where the subscript r means that the partial derivative must be taken at given material point r, not at given geometrical radius R. We have from (3.15)

$$- \frac{\partial \log T}{\rho\, \partial R} = \frac{1.8}{(\gamma' - 1)\rho R} \tag{5.41}$$

Similarly, from (5.28)

$$-\left(\frac{\partial \log T}{\partial t}\right)_r = \beta \frac{\partial \log p}{\partial t} = - \frac{1.2\ \beta}{t}$$

$$= - \frac{0.8}{t} \frac{\gamma' - 0.9}{\gamma'} \tag{5.42}$$

61

assuming the strong shock relation $p \sim t^{-1.2}$. The ratio (5.40) is then

$$- \rho \frac{dr}{dt} = \frac{0.8}{1.8} \frac{(\gamma' - 0.9)(\gamma' - 1)}{\gamma'} \frac{\rho R}{t} \tag{5.43}$$

Here we use the relation (3.10)

$$\rho = \frac{\gamma'}{\gamma' - 1} \frac{p}{H} \tag{5.44}$$

and find

$$- \rho \frac{dr}{dt} = \frac{4}{9} (\gamma' - 0.9) p \frac{R}{t} \frac{1}{H_1} \tag{5.45}$$

where H has been labeled H_1 because it refers to the radiating temperature. Here we may insert (3.30) and (3.31), viz.,

$$\frac{R}{t} = \frac{5}{2} \sqrt{2} \sqrt{\frac{p}{\rho_1}} \tag{5.46}$$

We may then compare the result with (5.18), the velocity of the cooling wave (setting $J_0 = 0$)

$$u = \frac{J_1}{H_0 - H_1} \tag{5.47}$$

The comparison gives

$$\frac{10 \sqrt{2}}{9} (\gamma' - 0.9) \frac{p^{3/2}}{\rho_1^{1/2}} = \frac{H_1}{H_0 - H_1} J_1 \tag{5.48}$$

62

Inserting (3.33) for J_1, and changing the unit of p from dynes/cm^2 to bars = 10^6 dynes/cm^2 we get

$$p_1^{3/2} = 570 \sqrt{\rho_0} \; \frac{9}{10\sqrt{2}} \; \frac{1}{\gamma'-0.9} \; \frac{T_1'^{17/3}}{T_c'^{5/3} - T_1'^{5/3}}$$

With $\rho_0 = 1.29 \times 10^{-3}$, $\gamma' = 1.15$ this becomes

$$p_1 = 14 \left(\frac{\rho_1}{\rho_0}\right)^{1/3} \frac{T_1'^{34/9}}{T_c'^{10/9}} \left[1 - \left(\frac{T_1'}{T_c'}\right)^{5/3}\right]^{-2/3} \tag{5.49}$$

Setting now $\rho_1 = \rho_0$ and choosing, as in Sec. 5d, $T_c' = 3.6$ and $T_1' = 1.08$ yields

$$p_1 = 5.0 \text{ bars} \tag{5.50}$$

Thus the critical pressure is 5 bars, which was the reason for the choice of this number at the end of Sec. 5d. There it was shown that 5 bars and $T_c' = 3.6$ leads to $T_1' = 1.08$ so that our numbers are consistent.

We had to rely on Brode's solution to find T_c for a given p; this could only be avoided by obtaining an analytic solution for the isothermal sphere which will be discussed in a subsequent paper. Apart from this our treatment is analytical, making use of the equation of state and the absorption characteristics of air.

f. Maximum Emission

In this section we consider Stage C I, i.e., the condition when the pressure is larger than p_a, (5.50). Then the radiating surface is in the adiabatic region described in Sec. 3c. The condition for its position is, (3.21), $\ell = R/50$. From Brode's curves, the position of a point of temperature T' near 1 is given approximately by

$$R = 0.78 \, Y^{1/3} \, T'^{-0.10} \, p^{-1/4} \tag{5.51}$$

This expression comes purely from the numerical calculation, except that the correct dependence on yield is inserted. Y is in megatons, p in bars, R in kilometers. Equation (5.51) holds from p = 5 to 100 bars within about 5%. The absorption coefficient is given in (4.10), which yields

$$\ell = \frac{1}{\mu} = \frac{2.7 \times 10^{-2}}{\rho_0} \left(\frac{\rho_0}{\rho}\right)^{1.3} T'^{-7}$$

$$= 8 \times 10^3 \, p^{-1.45} \, T'^{-4.9} \, \text{cm} \tag{5.52}$$

using the equation of state (4.11). Equating this to 1/50 of (5.51) gives

$$T'^{4.8} = 4.5 \, Y^{-1/3} \, p^{-1.20} \tag{5.53}$$

$$T' = 1.37 \, Y^{-0.07} \, p^{-0.25} \tag{5.54}$$

Thus the radiating temperature increases as the pressure decreases.

64

Since $p \sim t^{-1.2}$,

$$T' \sim t^{0.3} \tag{5.55}$$

i.e., the increase of temperature with time is fairly fast. This is entirely due to the "opening up" of the shock, i.e., the decrease in absorption with decreasing density (pressure).

For given pressure, the radiating temperature (5.54) is slightly higher for smaller yield, an effect which has been observed. A factor of 1000 in yield corresponds to a factor 1.6 in temperature, hence a factor 7 in radiation per unit area. The total radiated power (assuming black body) at given p is proportional to

$$R^2 T'^4 \sim Y^{2/3-0.26} p^{-2/3-1} \sim Y^{0.40} p^{-5/3} \tag{5.56}$$

The relatively low power of the yield is remarkable in this formula, which describes Stage C I. Since the total energy radiated should be approximately proportional to Y, the duration of Stage C I is then proportional to $Y^{0.60}$. The observed time to the second radiation maximum is about proportional to $Y^{0.5}$. Our theoretical dependence of T' on yield is therefore somewhat too strong. The time dependence of (5.56) is quite strong, about as t^2.

As we have shown in Sec. 5e, Stage C I ends when the pressure reaches 5 bars. For this value of p, and for $Y = 1$, (5.54) gives $T' = 0.92$. This is slightly less than the $T' = 1.08$ deduced in Sec. 5d for the same p and Y from the cooling wave. The discrepancy must be due to a small

inconsistency in our approximations.

In our one-dimensional theory, the end of Stage C I marks the maximum of radiation, both in temperature and total emission. In Stage C I the radiating temperature _increases_ with decreasing pressure, (5.54), because the material becomes more transparent. In Stage C II the reverse is the case, (5.39), because the material which has gone through the cooling wave becomes thicker with time, (5.32). This material provides opacity for the visible light from the fireball; since it becomes more opaque, the radiation must now come from a layer of smaller absorption coefficient, (5.35), and therefore of lower temperature. As (5.36) shows, the increase of thickness (t in the denominator) is more important than the continued decrease of density (factor $p^{1/3}$). These results will be modified in the three-dimensional theory, Sec. 6.

The maximum temperature has been calculated as $T' = 0.92$ or 1.08, from our two calculations; it is clearly close to 1, i.e., $10,000°$. This number is not too much out of line with observation considering that we have calculated a _maximum_. In fact, the transition from Stage C I to C II cannot be sudden as we have assumed; the cooling wave must begin gradually, and therefore the temperature peak which we have calculated will actually be cut off (Fig. 3). The observable maximum may easily be $1000°$ lower than our calculation.
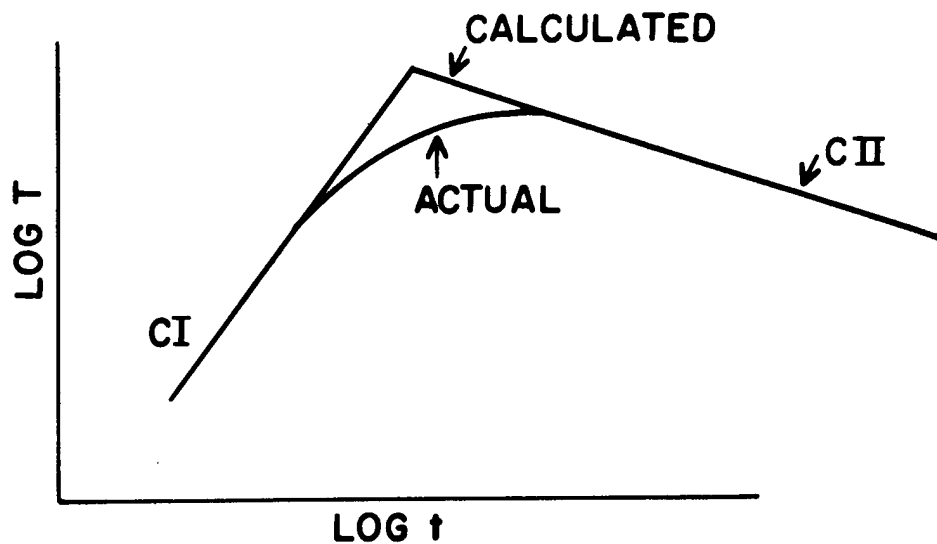
Fig. 3. The calculated increase in temperature in Stage C I, and decrease in Stage C II (straight lines), and the estimated actual behavior.

The radius of the radiating surface increases with time in Stage C I. Inserting (5.54) into (5.51) gives

$$R \sim Y^{0.34} \, p^{-0.225} \sim t^{0.27} \tag{5.57}$$

In Stage C II, the surface moves rather rapidly inward relative to the material, due to the cooling wave. In addition, for sea level explosions at least, the pressure is no longer much above ambient, so that the outward motion of the material slows down. Thus the geometric radius of the radiating surface no longer increases much, and soon begins to decrease. Therefore, the total radiation will reach its maximum at the same time as, or very soon after, the maximum of the temperature.

67

g. Weak Cooling Wave

In Stage C II the cooling wave dominates the radiation (Sec. 5d). In Stage C I the cooling wave also <u>exists</u>, because the energy of the radiation must be provided. However, the speed at which the wave proceeds inward is now governed by the adiabatic expansion, (5.45). In order to obtain the correct flux of radiation J_1 at the radiating surface, we must therefore use (5.18) in reverse: The temperature T_0 at the <u>inner</u> edge of the cooling wave (point B in Fig. 2) will regulate itself in such a way that (5.18) is satisfied, with u given by (5.45). Using (5.46), we thus get the condition

$$\frac{10\sqrt{2}}{9} (\gamma' - 0.9) \frac{p^{3/2}}{\sqrt{\rho_1}} = \frac{H_1}{H_0 - H_1} (J_1 - J_0) \qquad (5.58)$$

or solving for H_0 and inserting numbers:

$$\frac{H_0 - H_1}{H_1} \frac{1}{1 - J_0/J_1} = \frac{13}{\gamma' - 0.9} \sqrt{\frac{\rho_1}{\rho_0}} p^{-3/2} T_1'^4 \qquad (5.59)$$

Neglecting J_0, we find that H_0 increases rapidly as p decreases. We may insert (5.54); then the right hand side varies as $p^{-5/2} \sim t^3$. Thus the cooling wave starts very weak and then rapidly increases in strength. Its "head" (point B in Fig. 2) is at first close to its foot (point C). As time goes on, it moves more deeply into the hot material, eating up region II of Fig. 2. The energy which is made available for

radiation is essentially the difference $H_0 - H_1$: The material drops suddenly in temperature from T_0 to T_1 as the cooling wave sweeps over it, and the energy difference is set free for radiation.

The term J_0 depends on H_0, on p, and on the temperature gradient in the region inside the cooling wave (region II). If this region is adiabatic, the temperature gradient can be calculated from (3.15). Since J_1 is also related to the temperature gradient in the adiabatic region IV, the ratio J_0/J_1 tends to unity as $H_0 \rightarrow H_1$. Thus the left hand side of (5.59) will have a certain minimum value. This seems to indicate that there is no cooling wave at all until the pressure has fallen below a certain critical value. We have not investigated this point in detail. It is possible that it is simply related to the break-away of the luminous front from the shock wave, i.e., the beginning of Stage C.

Equation (5.59) describes the weak cooling wave in Stage C I no matter what the distribution of temperature in region II. The stage comes to an end when H_0 reaches the maximum possible value, H_c. Thereafter, the wave described by (5.59) becomes inadequate to supply the radiation energy: Since the enthalpy can no longer increase, the speed of the cooling wave has to increase. This speed is then given by (5.19), and Stage C II has begun.

6. EFFECT OF THREE DIMENSIONS

a. Initial Conditions and Assumptions

The fact that the fireball is spherical causes some deviations from the one-dimensional theory of Sec. 5. In this section we shall discuss Stage C II, the penetration of the cooling wave into the isothermal sphere, in three dimensions. Initially, we assume that the cooling wave has just reached the isothermal sphere; we call the corresponding time $t = t_a$, and the pressure is the critical pressure $p_a = 5$ bars derived in Sec. 5d. Subsequently, the mass of the isothermal sphere decreases due to the cooling wave.

We assume that the material, which is at temperature $T > T_m = 4000^\circ$ at the initial time t_a, will stay in this temperature range throughout Stage C II. This is reasonable because this material will be heated by the ultraviolet radiation coming from the inside, because of the strong absorption of air of medium temperature (3000 to 6000°) for UV (Sec. 4c). The UV heating is expected to compensate approximately the cooling due to adiabatic expansion of this material; this is confirmed by rough estimates of the heating and cooling. We do not know how the temperature is distributed in the "warm layer" between the radiating temperature T_1 and the temperature $T_m = 4000^\circ$; this could only be determined by a detailed calculation of the UV radiation flow in this region. We assume that the distribution is smooth, as it is in Stage C I, and that therefore the thickness of the "warm layer" in gm/cm^2 is directly proportional to the

required mean free path of visible light at the radiating temperature (also in gm/cm^2) which in turn determines T_1 itself.

We take the initial conditions from Brode,[8] using his curves at a time when the inside pressure is 4.1 bars, this being closest to $p_a = 5$ bars of all the curves he has published. This corresponds to a scaled (1-megaton) time $t_c = 0.325$ sec. At this time, important physical quantities are as given in Table VIII (dimensions scaled to 1 megaton). The last column of the table is not given by Brode but will be explained in Sec. 6c. In the table, we have defined a quantity proportional to the mass,

$$m = \rho_0^{-1} \int_0^{\infty} \rho(R)R^2 \, dR \qquad (6.1)$$

where R is measured in hundreds of meters. It is interesting that the mass of the warm layer is much (6.6 times) larger than that of the isothermal sphere. Its volume is about 2.4 times larger in Brode's calculations.

Table VIII. Conditions When Cooling Wave Reaches Isothermal Sphere, According to Brode

| | Isothermal Sphere | Warm Layer | |
		Brode	Sec. 6c
Outer radius, meters	385	577	438
Average density/ρ_0	0.79×10^{-2}	2.20×10^{-2}	11×10^{-2}
"Mass" m defined in (6.1)	0.150	0.99	0.99
Mean temperature T'	3.0	--	0.70

b. Shrinkage of Isothermal Sphere

We denote the "mass" of the isothermal sphere, as defined by (6.1), by m_1. Then this mass will decrease, due to the progress of the cooling wave inward, according to

$$\frac{dm_1}{dt} = - \frac{u}{\rho_0} R_1^2 \tag{6.2}$$

Note the ρ_0 in the denominator and the absence of the factor 4π, both due to the definition (6.1). The density of the isothermal sphere is nearly uniform and will be denoted by ρ_{is}. Initial values at time t_a will be denoted by a subscript a. The isothermal sphere expands adiabatically, hence

$$\rho_{is} = \rho_a \left(\frac{p}{p_a}\right)^{1/\gamma} \tag{6.3}$$

and therefore at any time t

$$\left(\frac{R_1}{R_a}\right)^3 = \left(\frac{m_1}{m_a}\right) \left(\frac{p_a}{p}\right)^{1/\gamma} \tag{6.4}$$

The speed of the cooling wave is given by (5.10), thus

$$u = \frac{J_1}{H_0 - H_1} \tag{6.5}$$

where J_0 has been set equal to zero because there is no appreciable flow

72

of radiation inside the sphere. H_0 is the enthalpy inside the sphere, which decreases adiabatically

$$H_0 = H_{0a} \left(\frac{p}{p_a}\right)^{(\gamma-1)/\gamma} \tag{6.6}$$

H_1 is the enthalpy at the radiating surface. It will be shown in Sec. 6c that the temperature T_1 is nearly constant with time, so that in good approximation H_1 and J_1 in (6.5) are constant. We shall also make the poorer approximation that $H_1 \ll H_0$. Then (6.5) and (6.6) give

$$u = u_a \left(\frac{p_a}{p}\right)^{(\gamma-1)/\gamma} \tag{6.7}$$

Inserting (6.4) and (6.7) into (6.2) and making the equation dimensionless,

$$\frac{d}{d(t/t_a)} \left(\frac{m}{m_a}\right) = -\frac{u_a t_a R_a^2}{\rho_0 m_a} \left(\frac{R_1}{R_a}\right)^2 \frac{u}{u_a}$$

$$= -3 \frac{u_a t_a}{\rho_a R_a} \left(\frac{m_1}{m_a}\right)^{1-1/3\gamma} \tag{6.8}$$

We define

$$x = \frac{t}{t_a}$$

$$y = \left(\frac{m}{m_a}\right)^{1/3}$$

$$f(x) = \frac{p_a}{p}$$

$$A = \frac{u_a t_a}{\rho_a R_a} \tag{6.9}$$

and obtain the simple differential equation

$$\frac{dy}{dx} = - A f(x)^{1-1/3\gamma} \tag{6.10}$$

which yields, together with the boundary conditions,

$$y = 1 - A \int_1^x f(x')^{1-1/3\gamma} \, dx' \tag{6.11}$$

The constant A can be determined from Sec. 5e. The condition there is

$$u_a = - \rho \frac{dr}{dt} \tag{6.12}$$

where ρ is the density <u>outside</u> the cooling wave. According to (5.44)

$$\frac{\rho}{\rho_a} = \frac{H_c}{H_1} \tag{6.13}$$

Then using (5.43)

$$\frac{u_a}{\rho_a} = \frac{H_a}{H_1} \frac{4}{9} \frac{(\gamma' - 0.9)(\gamma' - 1)}{\gamma'} \frac{R_a}{t_a} \tag{6.14}$$

Using $T_a' = 3.6$, $T_1' = 0.98$, $H \sim T^{5/3}$, we find $H_a/H_1 = 8.7$. Using further $\gamma' = 1.18$, A in (6.9) becomes

$$A = 8.7 \times \frac{4}{9} \times \frac{0.18 \times 0.28}{1.18} = 0.166 \qquad (6.15)$$

which is a pure number, and small: The calculation could be improved by not neglecting H_1 compared with H_a.

According to (6.11) the fireball is used up at the time x defined by

$$\int_1^x f(x')^{1-1/3\gamma} \, dx' = \frac{1}{A} = 6 \qquad (6.16)$$

This relation is valid (granted the approximations we have made) whatever the relation between pressure and time, $f(x)$. This generality is useful for sea level explosions, where p_a is only 5 times ambient pressure: The relation between p and t can then be taken from a machine calculation (or observation).

For higher altitude, let us say h > 10 km, $p_a = 5(\rho_1/\rho_0)^{1/3}$ is sufficiently above the ambient pressure, ρ_1/ρ_0, so that the shock is still strong and we may use

$$f(x) = x^{1.2} \qquad (6.17)$$

Then (6.11) becomes

$$y = 1 - A \frac{x^{2.2-0.4/\gamma} - 1}{2.2 - 0.4/\gamma} \qquad (6.18)$$

From $\gamma = 1.18$,

$$y = \frac{12.2 - x^{1.86}}{11.2} \qquad (6.19)$$

and the isothermal sphere disappears for

$$x_2 = 12.2^{1/1.86} = 3.84 \qquad (6.20)$$

For these higher altitudes, then, the time when the isothermal sphere disappears is a fixed multiple of the time when it is first reached by the cooling wave. This multiple depends only on γ, and on the ratio H_c/H_1 of internal to external enthalpy at time t_a. The pressure at the time x_2 is

$$p_2 = p_a x_2^{-1.2} = 1.0 \left(\frac{\rho_1}{\rho_0} \right)^{1/3} \qquad (6.21)$$

For sea level, $f(x)$ increases more slowly (the pressure decreases more slowly) with time; hence it takes somewhat longer to use up the isothermal sphere. Conversely, the pressure at the time $t_2 = t_a x_a$ will have decreased by a smaller factor from p_a.

For the simple case of higher altitude, we can use (6.19) to calculate the fraction of the mass y^3 which will still be in the isothermal

sphere, its radius R_1/R_c, and other physical data. Some of these are given in Table IX. It is seen from the table that the mass decreases, first fairly uniformly and rapidly (as if it would go to zero at x = 2.8), then more slowly (because it is proportional to y^3), while the radius first expands slightly, then shrinks slowly and at the end very rapidly. The latter phenomenon, the rapid shrinking of the apparent fireball, may not be observable because the bomb debris becomes visible and is likely to be still opaque. But some shrinkage of the fireball should be open to observation.

Table IX. Development of Isothermal Sphere and Warm Layer
due to Cooling Wave

$x = t/t_a$	1.0	1.2	1.5	2.0	2.5	3.0	3.5	3.84
	1	0.964	0.899	0.766	0.599	0.402	0.188	0
$m_1/m_a = y^3$	1	0.895	0.726	0.450	0.215	0.065	0.0066	0
R_1/R_a	1	1.029	1.031	0.970	0.818	0.584	0.287	0
R_2/R_a	1.137	1.194	1.248	1.296	1.326	1.362	1.426	1.483
L'	0.137	0.129	0.126	0.129	0.150	0.180	0.214	0.247

The last two lines of Table IX will be explained in Sec. 6c.

c. The Warm Layer

We want to assume that the outer edge of the warm layer, the 4000° temperature level, stays fixed in the material (Sec. 6a). We wish to calculate the thickness of the warm layer in gm/cm^2,

$$L = \int_{R_1}^{R_2} \rho(R) \, dR \qquad (6.22)$$

where R_2 is the outer edge of the layer. The original mass of the warm layer m_w is much larger than that of the isothermal sphere

$$m_w/m_a = B = 6.6 \qquad (6.23)$$

At a later time, the mass of the warm layer is then

$$m_2 = m_a(B + 1 - y^3) \qquad (6.24)$$

It does not change much.

The temperature in the warm layer goes from 10,000 to 4000°. For simplicity we assume that the density corresponds to the average temperature of 7000°. Then, at the initial pressure used in Table VIII, $p_a = 4.1$ bars, the density of the warm layer is $\rho_w = 11 \times 10^{-2} \rho_0 = 14\rho_a$. This is much higher than in Brode's calculations, Table VIII: In his calculations, the cooling wave has not reached the isothermal sphere; with our assumptions it has. The difference is due to the different opacities assumed; it has the consequence that our warm layer is geometrically much thinner than his (Table VIII, last column). Subsequently the density decreases with pressure, not adiabatically but isothermally; in accord with Gilmore's formula (3.13), we assume

$$\rho_2 = \rho_w \left(\frac{p}{p_a}\right)^{1.11} = \rho_a C \left(\frac{p}{p_a}\right)^{1.11} \qquad (6.25)$$

with C = 14.

On this basis we calculate the outer radius R_2 of the warm layer and find

$$R_2^3 = R_1^3 + R_a^3 \frac{B + 1 - y^3}{C} [f(x)]^{10/9} \qquad (6.26)$$

Using (6.17) we can then calculate R_2/R_a. We give this quantity in the second last line of Table IX. In the last line, we have given the material thickness of the warm layer, in relative units,

$$L' = \frac{\rho_2}{\rho_a} \frac{R_2 - R_1}{R_a} \qquad (6.27)$$

It is seen from the table that R_2 increases only slowly; the main change in $R_2 - R_1$ at later times is therefore due to the decrease of R_1. The material thickness L' first decreases very slightly; this continues about as long as R_1 increases, and is due to the fact that about the same mass of warm material gets distributed over a larger area. Later on, L' increases while R_1 decreases. Until x = 2.5 the change of L' remains less than 10%, and after x = 2.5 the calculation is probably meaningless because the bomb debris comes into view. Therefore, we may assume L' constant, and thus the optical mass absorption coefficient (in cm^2/gm) at the radiating layer will also be constant. In contrast with this

result of the three-dimensional considerations, the one-dimensional formula (5.35) yields a decrease of μ/ρ as t^{-1}.

Using (5.33), a constant mass absorption coefficient requires

$$T'_1 \sim p^{-1/3n} \sim p^{-1/20} \tag{6.28}$$

Thus in three dimensions, the <u>temperature continues to increase slowly</u> after the cooling wave reaches the isothermal sphere. If we assume that times up to $x = 2.5$ in Table IX are significant, the pressure decreases by about a factor of 3 in Stage C II, and the temperature of the radiating layer increases by about 5% according to (6.28). The radiated power, being proportional to $R_1^2 T_1'^4$, may increase by about 10% up to $x = 2$, and then decreases due to the shrinkage of the radiating surface.

One prediction of this theory is that the temperature, as well as the radiated power, has a rather <u>flat</u> second maximum while the isothermal sphere radiates away its energy. The slow variation of T_1 justifies the treatment of J_1 as constant in Sec. 6b.

7. TRANSPARENT FIREBALL (Stage D)

After the isothermal sphere has been eliminated by the cooling wave, the fireball is transparent if we neglect the effect of the bomb debris. At this time the pressure is given by (6.21), the average temperature of the "warm" region is about 7000°, and the corresponding density is about

$$\frac{\rho_b}{\rho_0} = 2.3 \times 10^{-2} \left(\frac{\rho_1}{\rho_0}\right)^{0.37} \qquad (7.1)$$

If we assume that the radius R_a of the isothermal sphere scales with $\rho_1^{-1/3}$ (which may be wrong) the radius of the warm sphere is now

$$R_b = 570 \left(Y \frac{\rho_0}{\rho_1}\right)^{1/3} \text{ meters} \qquad (7.2)$$

where Y is in megatons. Therefore, along a radius, the amount of warm material is about

$$\rho_b R_b = 1.7 \ Y^{1/3} \ \text{gm/cm}^2 \qquad (7.3)$$

almost independent of ambient air density.

Taking $\rho_b/\rho_0 = 10^{-2}$ (which corresponds to $\rho_1/\rho_0 \approx 10^{-1}$) and an average temperature of 7000°, Meyerott's tables give for the visible:

$$\frac{\mu}{\rho} \approx 0.4 \ \text{cm}^2/\text{gm} \qquad (7.4)$$

so that the radius represents 0.7 optical mean free path at 1 megaton. This is nearly transparent, and the fireball becomes rapidly more transparent as it cools down by further emission of radiation. The emission of radiation is then proportional to the opacity; for each material element,

$$\frac{dE}{dt} = - 4KaT^4 \tag{7.5}$$

where a is the Stefan-Boltzmann constant and K the opacity in cm^2/gm,
i.e., the absorption coefficient averaged over a Planck spectrum (dis-
regarding spectral regions which are still black). Since K increases
rapidly with temperature, the hottest region near the center will cool
fastest, so that the temperature tends to become more uniform.

For the same reason, the radiative cooling will effectively stop at
a temperature of about 5000°. At this temperature and $\rho = 0.01\rho_0$, it
takes about 5 seconds to cool the fireball by 10%. At 4000°, this takes
about 200 seconds. Gilmore[25] has calculated curves of cooling times for
transparent bodies at various densities as a function of the final temper-
ature.

Depending on the ambient density, the pressure may or may not have
decreased to ambient pressure when the temperature has decreased to 5000°.
Even if it has not, the subsequent adiabatic expansion will not lower the
temperature much further. (Our theory is not applicable to very low
ambient densities because there the isolation of isothermal sphere from
the outside never takes place. Probably the limit of applicability is
about $\rho_1/\rho_0 = 10^{-2}$. Therefore, and because of the small value of $\gamma - 1$,
expansion cannot be large.) Therefore, after both radiation and hydro-
dynamics have effectively stopped, the fireball is left at a temperature
not much below 5000°.

Any further cooling can only be achieved by the rise of the fireball

due to its bouyancy, and the turbulent mixing associated with this rise. This is a slow process, taking tens of seconds.

Since the emission is now proportional to the absorption coefficient, the molecular bands will now appear in emission while in earlier stages they appear in absorption. This has been observed.

The debris, at the center of the fireball, contains metals and therefore is likely to be opaque at lower temperatures. Therefore the debris may well be opaque after all the air has become transparent. The debris usually has a ragged shape due to Taylor instability. Recently, Longmire[26] has given a tentative, quantitative theory of this instability in debris expansion. Because of its higher opacity, the debris may cool to a lower temperature than the surrounding air.

REFERENCES

1. H. A. Bethe and E. Teller, 1942 (unpublished).

2. R. E. Marshak, Report LA-230, 1945.

3. J. O. Hirschfelder and J. L. Magee, Chap. 3 in Report LA-2000, 1947.

4. Samuel Glasstone, Ed., "Effects of Nuclear Weapons," Department of Defense and Atomic Energy Commission, U. S. Government Printing Office, 1962.

5. H. E. DeWitt et al., Report LAMS-1935, 1955.

6. B. E. Freeman, General Atomic Report GAMD-4106, 1963 (classified).

7. H. L. Brode and F. R. Gilmore, Rand Report RM-1983, 1957 (classified).

8. H. L. Brode, Rand Report RM-2248, 1959 (classified).

9. H. L. Brode and R. E. Meyerott, Rand Report RM-1851, 1956 (classified).

10. Zel'dovich, Kompaneets, and Raizer, JETP 7, 882 and 1001 (1958) (English translation).

11. H. L. Brode, Rand Reports RM-2247 and RM-2249, 1958 (classified).

12. F. R. Gilmore, Rand Report RM-2959, 1962 (classified).

13. F. R. Gilmore, Rand Report RM-1543, 1955.

14. Hilsenrath, Green, and Beckett, Nat. Bur. Standards, ASTIA Document AD-96303, 1957.

15. Armstrong, Sokoloff, Nicholls, Holland, and Meyerott, J. Quant. Spectry. Radiative Transfer 1, 143 (1962).

16. Meyerott, Sokoloff, and Nicholls, Geophysical Research Papers, No. 68, Geophysics Research Directorate, Bedford, Mass., 1960.

17. B. Kivel and K. Bailey, Avco-Everett Research Note 43, 1957.

18. R. L. Taylor, J. Chem. Phys. _39_, 2354 (1963); also R. L. Taylor and B. Kivel, J. Quant. Spectry. Radiative Transfer _4_, 239 (1964).

19. F. R. Gilmore and A. L. Latter, Rand Report RM-1617, 1956 (classified).

20. W. Karzas and A. L. Latter, unpublished.

21. F. R. Gilmore, curves and opacities and effective opacities as function of temperature and density, informal publications by the Rand Corporation; also Reports RM-2959, 1962, and RM-3571, 1963 (classified).

22. J. C. Stuart and K. D. Pyatt, Jr., Report SWC-TR-61-71, Vols, I, II, and III, 1961.

23. F. R. Gilmore, Rand Report RM-3997-ARPA, 1964.

24. Keck, Allen, and Taylor, Avco-Everett Research Report 149, 1963.

25. F. R. Gilmore, informal publication from Rand Corporation.

26. C. Longmire, (private communication).